

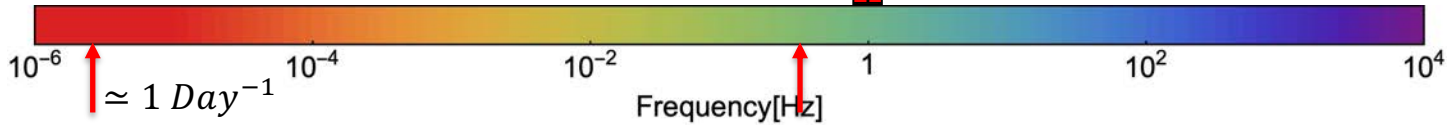
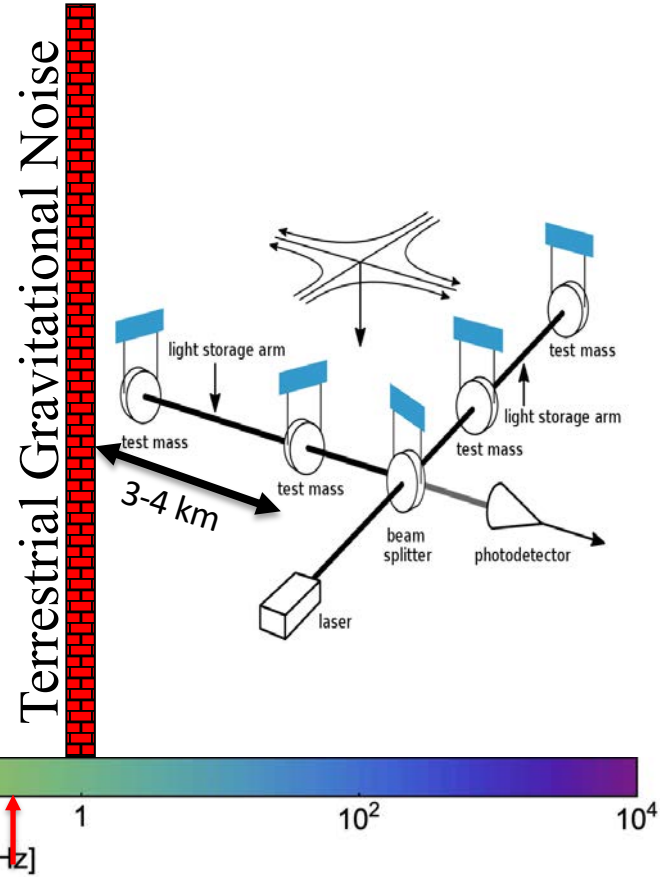
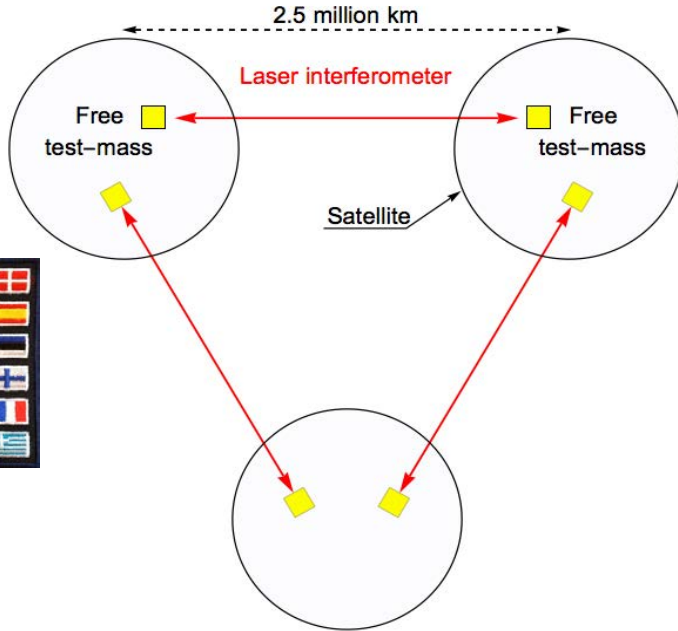
Space borne Gravitational Wave observatories. LISA Pathfinder, LISA and beyond

Stefano.Vitale@unitn.it

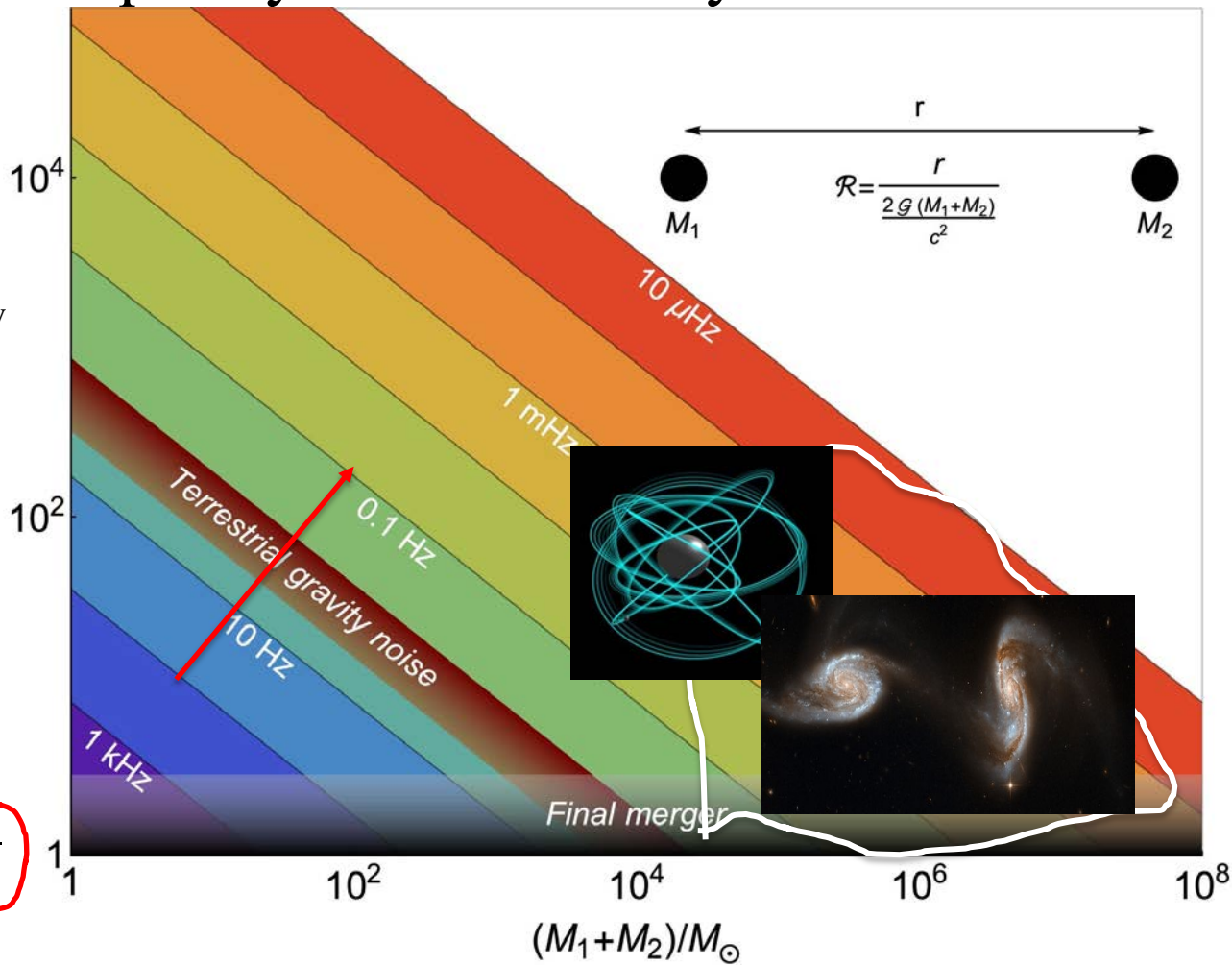
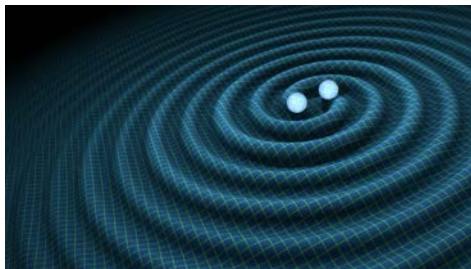
Università di Trento, Istituto Nazionale di Fisica

S. Vitale Nucleare and Agenzia Spaziale Italiana

LISA: the quest for low-frequency GW



Low frequency GW astronomy



- Binaries are nearly Keplerian, frequency of wave twice frequency of revolution

$$f_{GW} = \frac{1}{\pi} \sqrt{\frac{G(M_1 + M_2)}{r^3}} \quad \mathcal{R}$$

- Separation normalized to Schwarzschild radii:

$$\mathcal{R} = \frac{r}{\left(\frac{2G(M_1 + M_2)}{c^2}\right)}$$

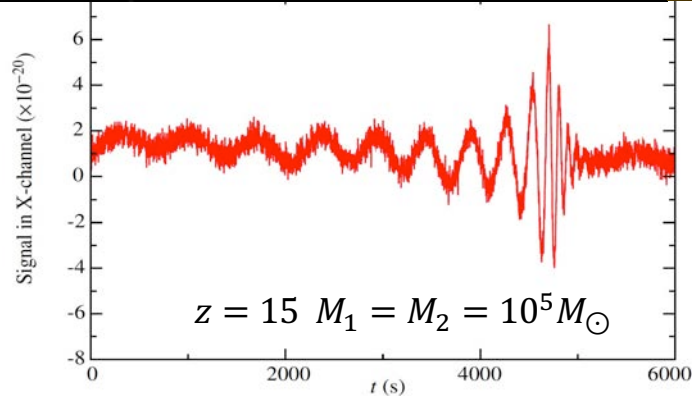
($\mathcal{R} \rightarrow 1 \simeq$ final merger)

- Frequency decreases with both mass and \mathcal{R}

$$f_{GW} = \frac{c}{\pi\sqrt{2} R_{\odot}} \left(\frac{M_1 + M_2}{M_{\odot}}\right)^{-1} \mathcal{R}^{-\frac{3}{2}}$$

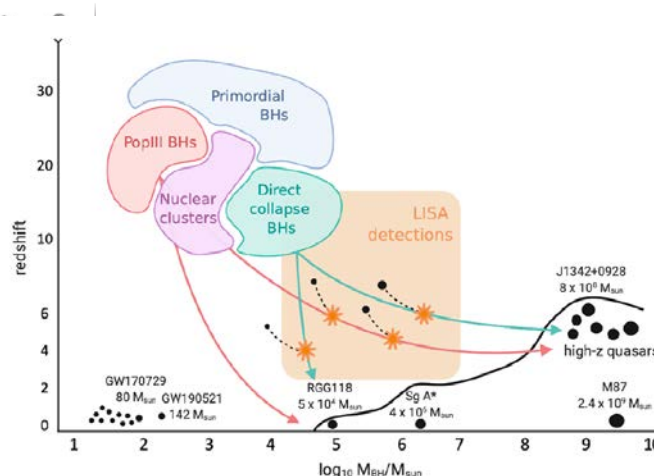
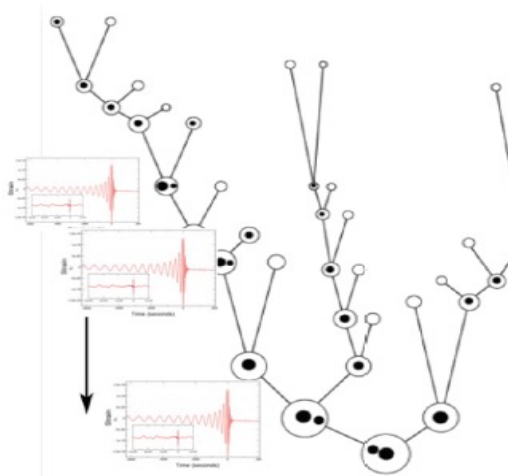
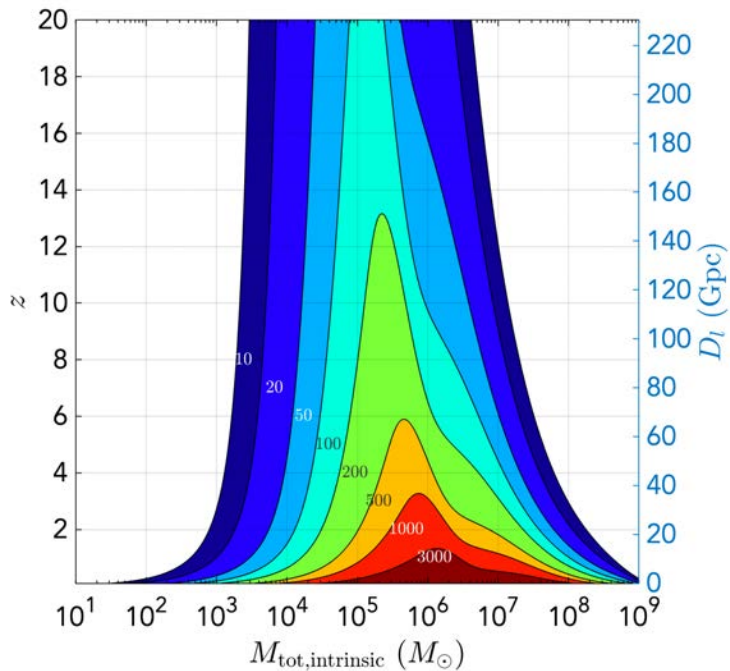
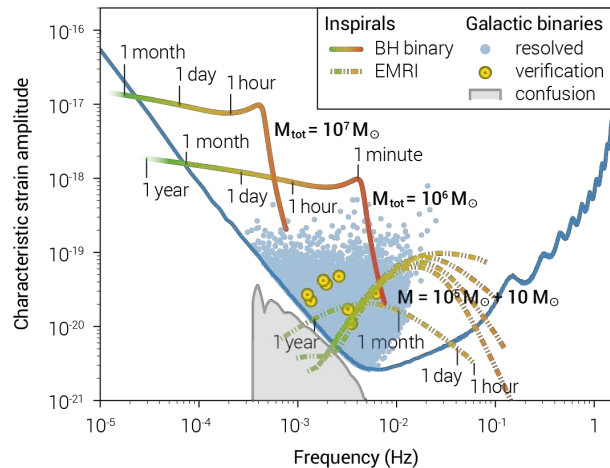
Supermassive BH mergers: the brightest sources

- Wave amplitude scales with $M_1 \times M_2$: detectable “everywhere” in the universe



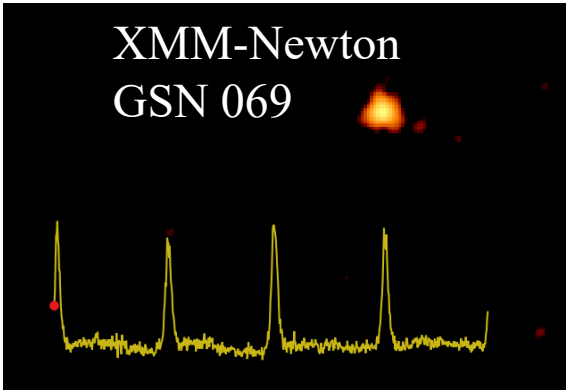
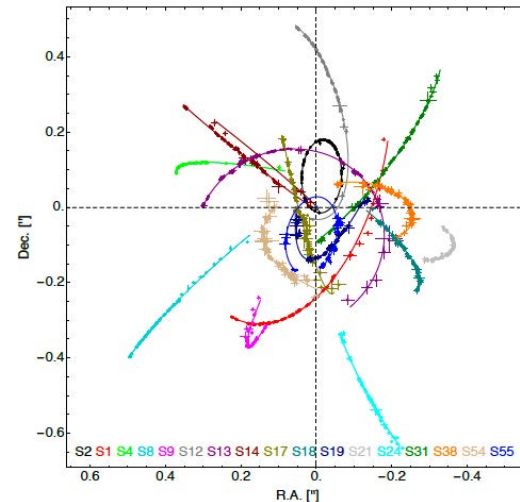
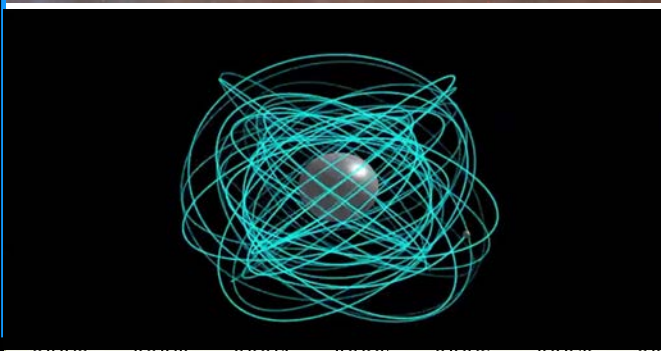
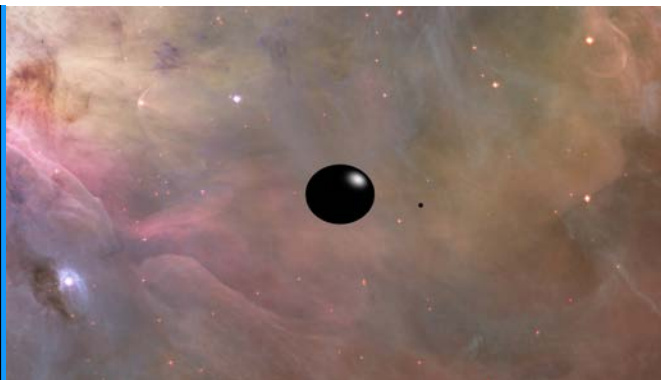
Supermassive BH mergers: the brightest sources

- Detectable “everywhere” in the universe
- Sooner or later frequency crosses LISA band : cosmological stratigraphy



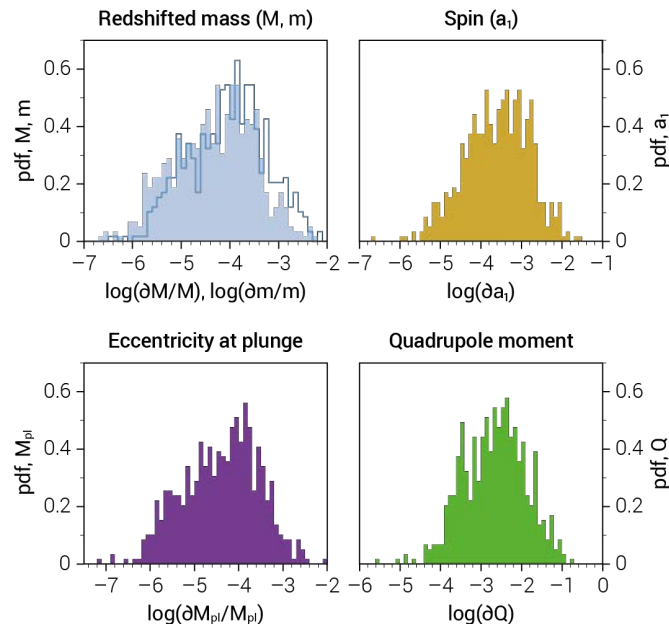
Extreme Mass Ratio Inspirals

- Inspiral of stellar-mass compact object (CO) into massive black hole (MBH): Hills & Bender 95
 - ✦ MBH mass $10^4 < M/M_{\odot} < 10^7$
 - ✦ Up to 10^4 - 10^5 cycles in band
 - ✦ If CO is a white dwarf, possible electromagnetic counterpart (Zalamea+10)
- Gravitational waves encode precise information on CO and MBH:
 - ✦ $M_{\text{BH}}(1+z)$, a_{BH} measurable to extreme precision
 - ✦ Detectable to $z \sim \text{few}$; sky localization ~ 1 - 10 deg^2 (Babak+17)
- Precise mapping of MBH spacetime
 - ✦ MBH multipole measurement \rightarrow test of no-hair theorem (Ryan 95)



EMRIs as a GRG lab

- The no-hair theorem: spacetime around BH determined by mass and spin
- No deformability
- Quadrupole moment measured at 0.1 % - 0.01 %
- Inconsistency with Kerr multipole structure allows to discriminate:
 - Strong environmental perturbation
 - New type of exotic compact object consistent with General Relativity: boson star, horizonless objects, non-Kerr axisymmetric geometries....
 - Failure in General Relativity itself: dynamical Chern-Simons, scalar-tensor theories, braneworld models, theories with axions, constraints within parametrised models...

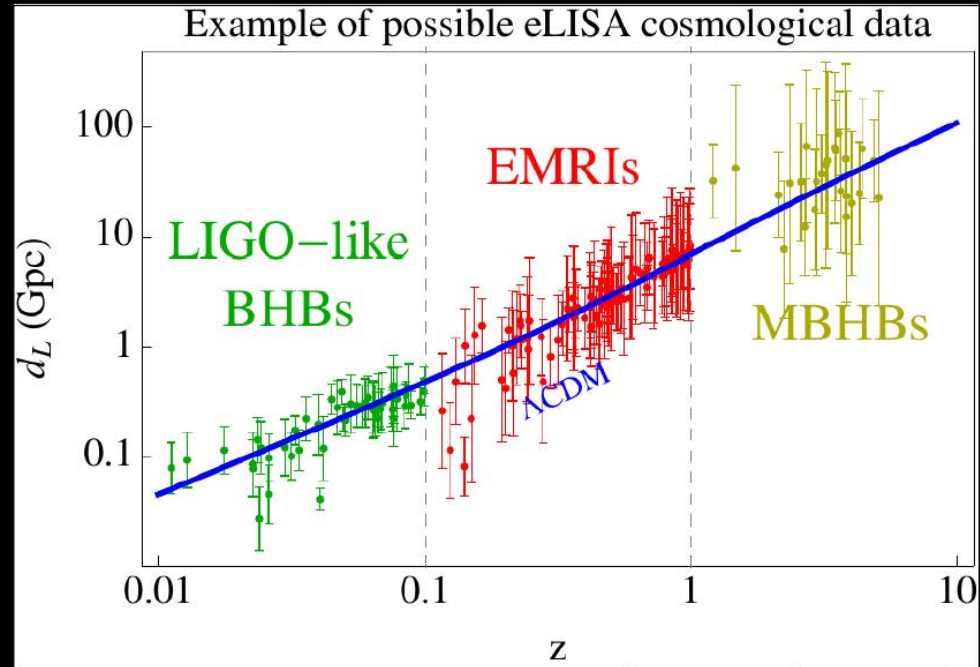


- GW from chirping binary systems are standard sirens: *absolute* luminosity distances D_L from period P and amplitude h :

$$D_L \propto \frac{cP\dot{P}}{h}$$

- GW *do not measure* redshift z . $D_L(z)$ requires identification of e.m. counterpart.

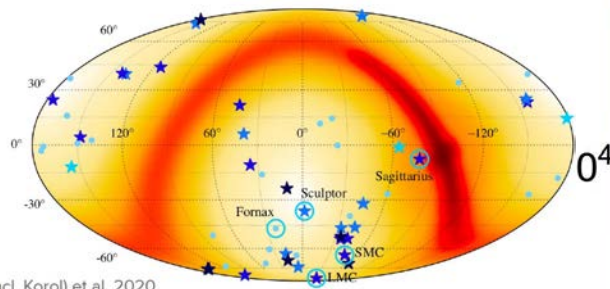
Cosmology with gravitational waves



(Courtesy of N. Tamanini)

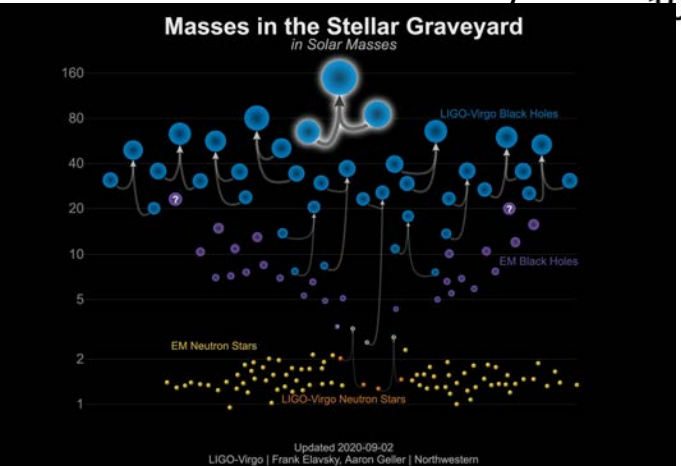
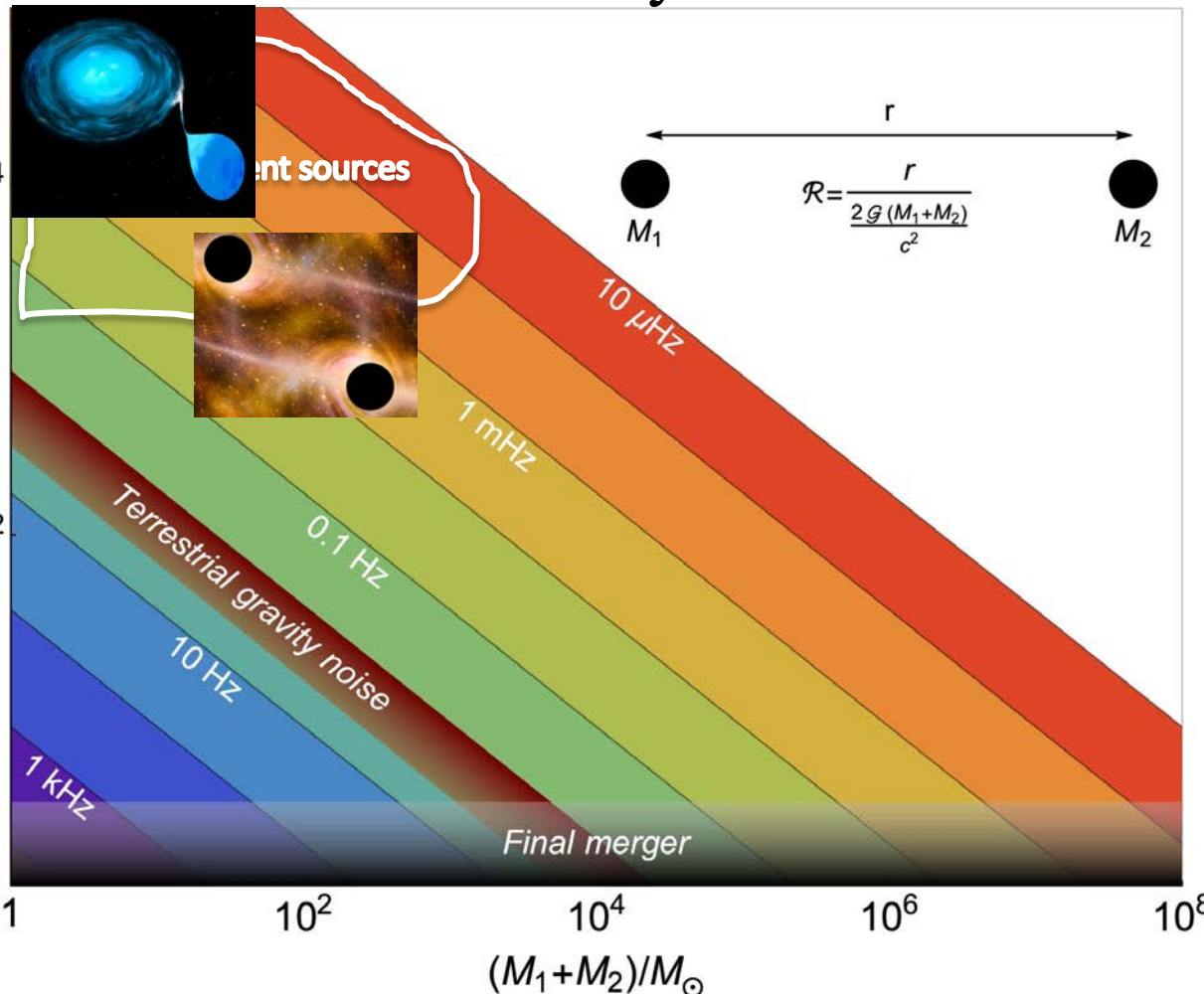
Different GW sources will allow an independent assessment of the geometry of the Universe at all redshifts.

Non-transient GW astronomy



Roebber (incl. Korol) et al. 2020

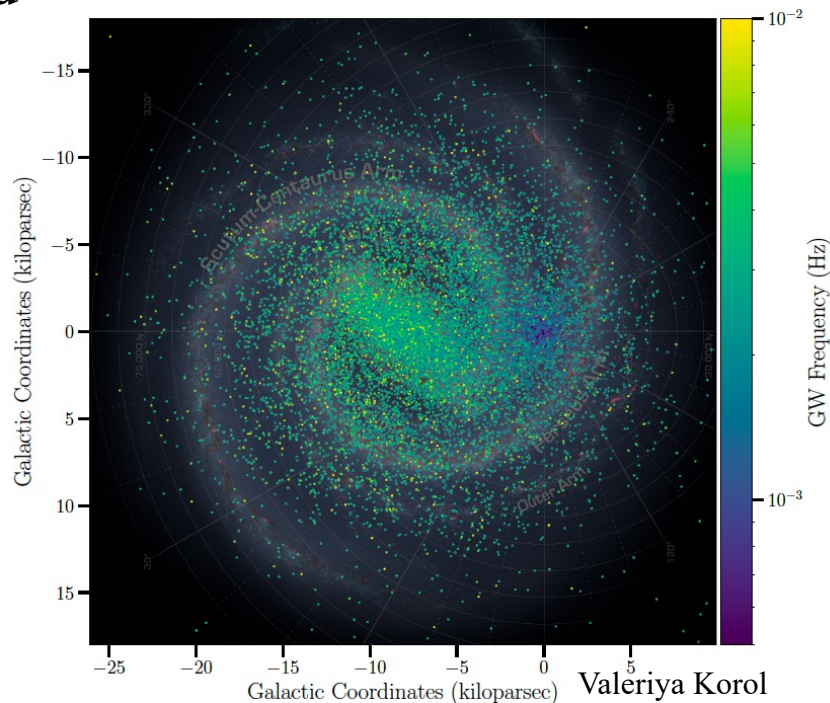
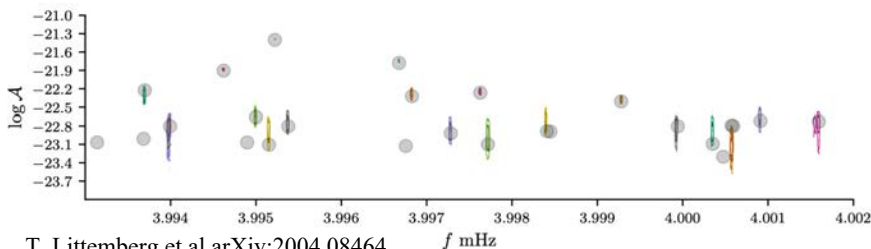
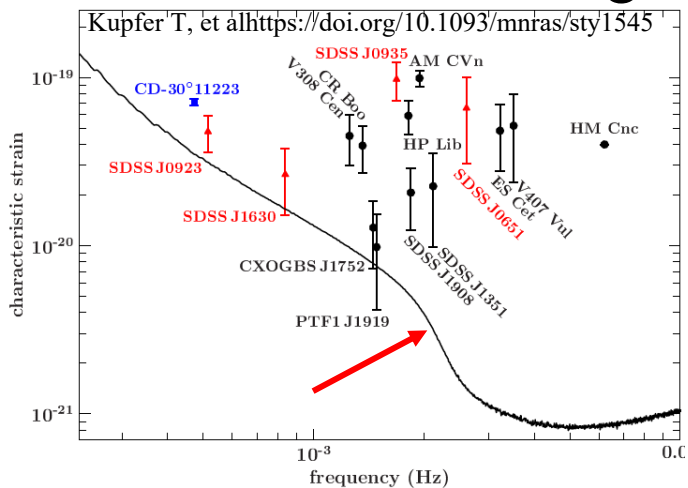
- GW-binary astronomy of local group
- BH multi-band astronomy



Updated 2020-09-02
LIGO-Virgo | Frank Elavsky, Aaron Geller | Northwestern

The high \mathcal{R} end: the GW Milky Way

- Tens of thousand of discernible sources
- Plus a stochastic foreground

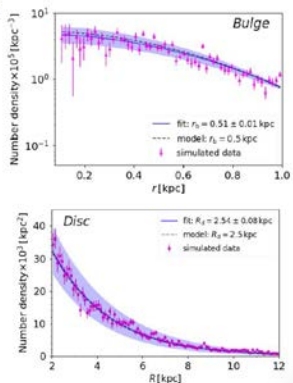


The shape of the Milky Way's components

The spatial distribution of DWDs with measured distances (several thousand) constrains:

- Bulge scale radius to 2%
- Disc scale radius to 3%
- Disc scale height to 16%

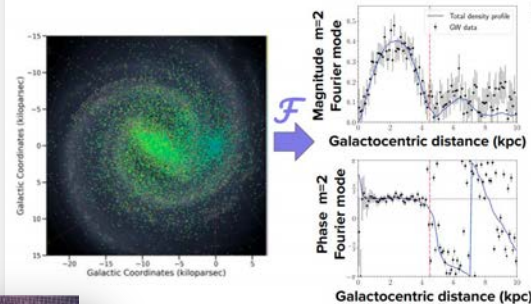
Korol et al 2019
See also Adams et al. 2012



Expectations

Structural parameters of the central bar

Fourier transformation of the DWD spatial distribution can reveal shape of the bar.



Specifically, it will constrain:

- axis ratio to 10%
- length to < 1%
- orientation angle to < 1°

(Wilhelm, Korol et al. 2020)



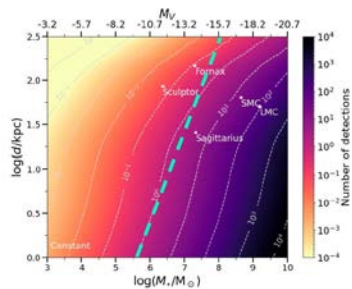
The detection of circumbinary exoplanets

Camilla DANIELSKI



Discovering Milky Way satellites in gravitational waves

- Satellites with stellar mass $> 10^6 M_\odot$ host detectable LISA sources
- LISA detections can inform us about the total stellar mass and star formation history of the satellites
- Discovery of satellites invisible to electromagnetic observatories

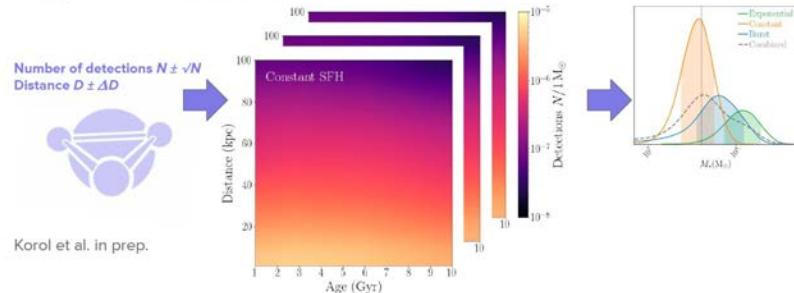


See talk by Riccardo Buscicchio

Korol et al. 2020; Roebber et al. (incl.Korol) 2020
See also Lamberts et al. 2019

Weighing Milky Way satellites

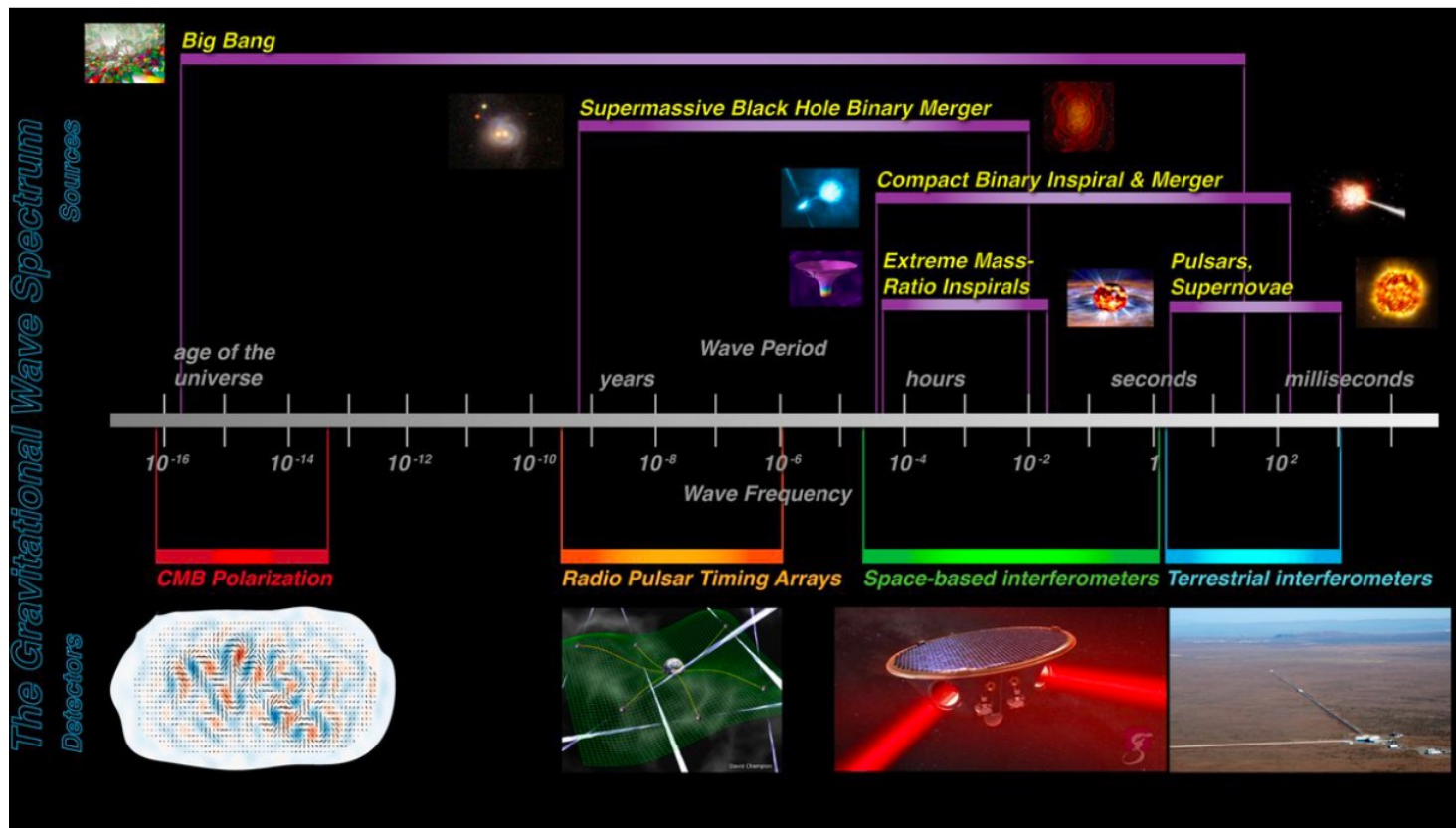
By exploiting our models we can recover the satellite's total stellar mass: to within a factor two if SFH is known and to an order of magnitude when marginalising over different SFH models. If no detections are identified with the satellite we can still place an upper limit on its stellar mass.



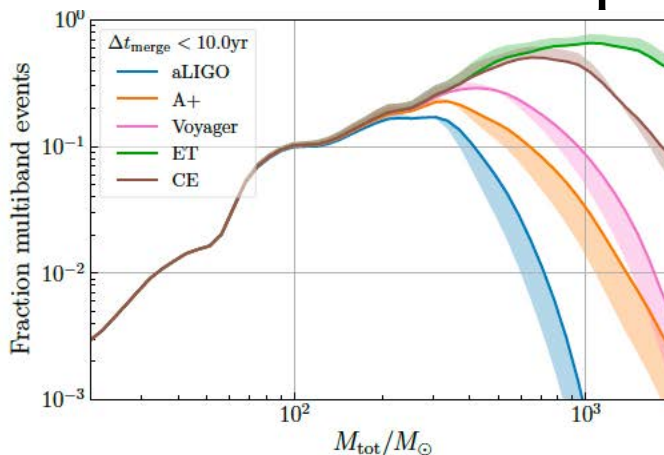
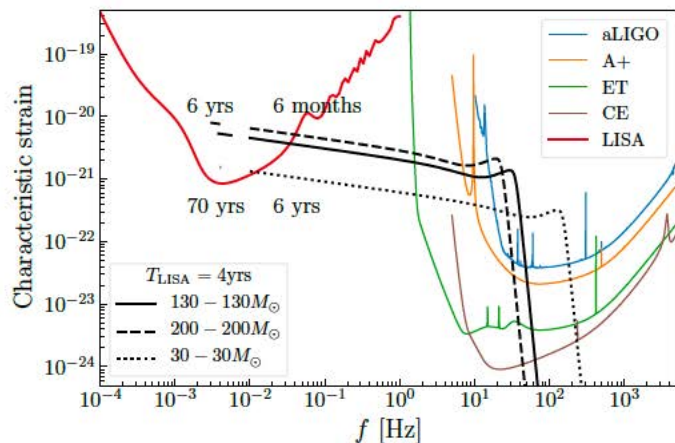
Korol et al. in prep.

S. Vitale

Multi-band GW astronomy



Multi-band GW astronomy and fundamental physics



Joint observation greatly improves measurement of deviation from GR

S. Datta et al arXiv:2006.12137v1 [gr-qc] 22 Jun 2020

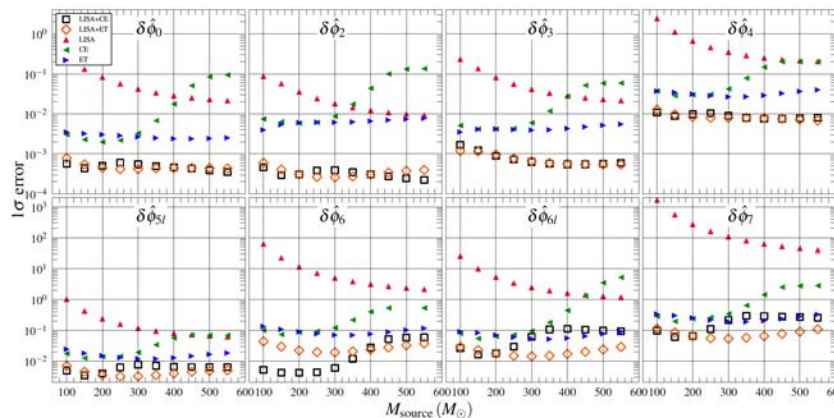
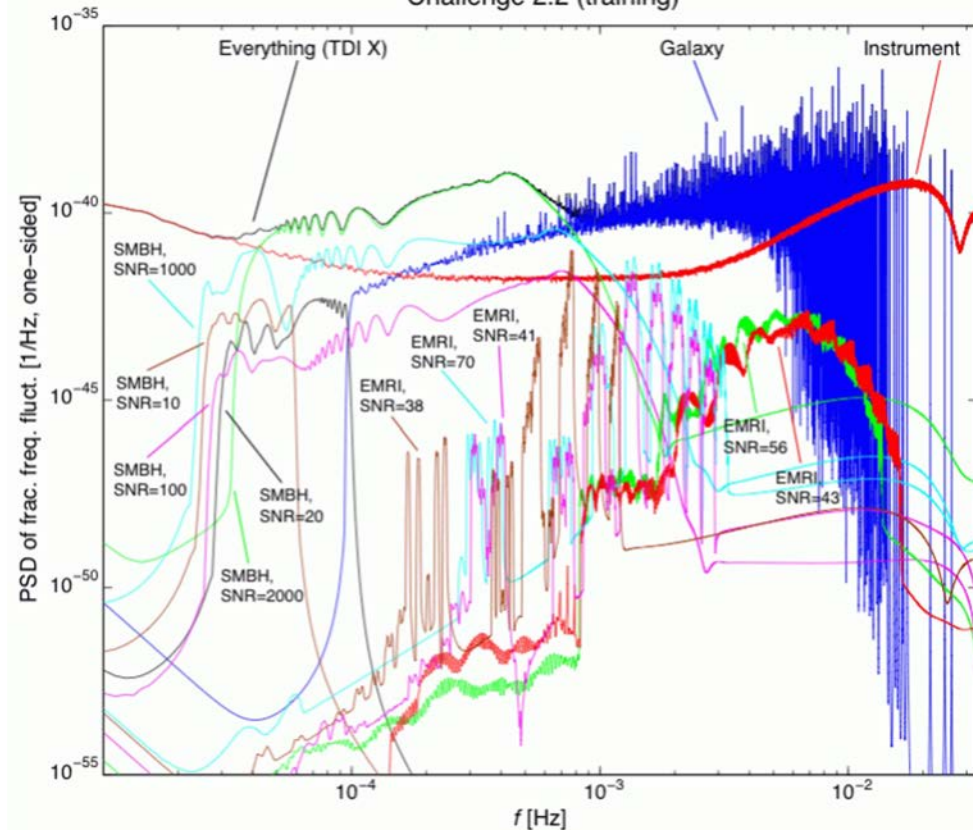


FIG. 3. Top panel shows bounds on deformation parameters at OPN to 2PN, as a function of total mass in source frame. Bottom panel shows the same but for deformation parameters at 2.5PN to 3.5PN. All the systems have mass-ratio $q = 2$, dimensionless component spins $\chi_1 = 0.2$ and $\chi_2 = 0.1$, and luminosity distance $D_L = 1$ Gpc.

Data analysis a formidable challenge

Challenge 2.2 (training)



LISA Data Challenge 2b: Spritz

We are glad to announce the release of several datasets in the second LISA Data Challenge, codenamed **Spritz**.

The purpose of this challenge is to address for the first time the realistic instrumental and environmental noise. The datasets are rather easy in the astrophysical content, moreover, the training data contain the sources that were used in the Sangria training dataset. If you are new to the Challenges, we strongly advise that you first complete the first data challenge **Radler** before moving to **Spritz**, specifically, challenges containing the merger of massive black hole binaries (MBHBs) and verification Galactic binaries.

The training **Spritz** data contain three sets. All three datasets were generated with the `r` pipeline used in the **Sangria** production. All GW sources follow conventions described in the `r` documentation and the same models (PhenomD for MBHB and Taylor-expanded for Galactic binaries). We have varied the noise level (assuming the same acceleration and optical mer spacecraft) within the same prior as in Sangria. Noise levels are given in the training data.

Features common to all datasets.

For the first time, we have used second-generation Michelson TDI combinations, expressed as fractional frequency deviations, at 5-second cadence. We have used a Keplerian model for the data contain scheduled gaps of 7 hours duration each, distributed with intervals between 10 and 15 days. We have included noise from the unresolved population of Galactic binaries with SNR=7 with respect to the total noise budget. We have included laser frequency noise, which is strongly dominant at low frequencies. The training datasets also contain partial versions of the `r` pipeline used to retrieve the total signal: with and without `r` artifacts (including gaps, glitches and non-stationary noise). The `r` glitch files used as input to the simulator are given, to facilitate the analysis.

MBHBs in Spritz data.

We have two datasets with merging MBHBs. (i) Dataset with a loud (SNR ~2000) GW signal, lasting for about 31 days. The signal is expected to be detectable a few weeks before the merger and, therefore, is suitable for testing low-latency algorithms. We have added three short loud glitches distributed in the inspiral, late inspiral and near merger parts of the signal. (ii) Dataset with a quiet (SNR ~100) GW signal lasting for one week, with several hour-long glitch placed near the merger. Parameters of both MBHBs are available in the training data, as well as the information about detected glitches injected in the two MBHB datasets correspond to events detected and fitted during the LISA Pathfinder operations (*Phys. Rev. Lett.* 120, 061101).

Verification GBs in Spritz.

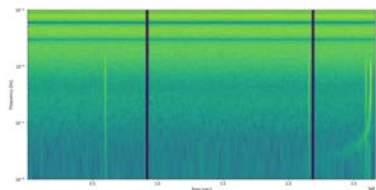
A 1-year long dataset contains 36 verification binaries, with parameters available in the same data file. We have placed glitches according to a Poisson distribution with a rate of 4 glitches per day, whose model is described in the Spritz documentation.

The LDC working group encourages you to conduct their own analysis using algorithms of their choice. We would like to see you join them to do so, e-mail us so we can pair you appropriately. Of course, you may organize to work on your own, or with your collaborators. For usage tracking purposes, we request that you set up a login for this website before downloading the datasets (your LDC-1 login will work fine). Please **submit your results by October 1st, 2022**, using the **submission interface** and format to be found on this website. Plan to include a description of your methods (or a link to a methods paper) with your submission. We would also greatly appreciate it if you were to share your code (e.g., on GitHub, or on our GitLab). To simplify a bit your life we have made several tutorials which, we hope, you will find useful: Tutorial notebooks link, LISANode simulation model.

While we did our best to check the datasets for correctness, small problems or inconsistencies may have escaped us. The best way to validate the data is to analyze it, so let us know of any problems!

- [Log in to download »](#)
- [LDC-2 documentation »](#)
- [Log in to get LDC-2 code »](#)
- [Ask for help »](#)

<https://lisa-ldc.lal.in2p3.fr>



Spectrogram of the 1st MBHB dataset, with a loud signal at day 30, 3 glitches at the beginning, middle and end of the time series, and 2 gaps seen as deep blue chunks.



Interesting reading

Astrophysics with LISA

Cosmology with LISA

Contents

General Introduction	3
I Stellar Compact Binaries and Multiples	5
1.1 Introduction and Summary	6
1.2 Classes of LISA binaries	8
1.2.1 Known binaries — LISA verification sources	8
1.2.2 Detached binaries	13
1.2.2.1 WD+WD systems	13
1.2.2.2 NS+WD and BH+WD systems	14
1.2.2.3 NS+NS systems	15
1.2.2.4 BH+NS and BH+BH systems	16
1.2.2.5 Stochastic background	17
1.2.3 Interacting binaries	17
1.2.3.1 AM CVn binaries (AM Canum Venaticorum binaries — accreting WDs)	17
1.2.3.2 UCXBs (ultra-compact X-ray binaries)	19
1.2.4 Other potential sources	20
1.2.4.1 Helium-star binaries	20
1.2.4.2 Period bouncing CVs	22

arXiv:2204.05434v1 [astro-ph.CO] 11 Apr 2022

Contents

1 Introduction	8
2 Tests of cosmic expansion and acceleration with standard sirens	11
2.1 Introduction	11
2.2 Standard sirens	11
2.2.1 Bright sirens: MBBHs with electromagnetic counterpart	12
2.2.2 Dark sirens: SOBBH, EMRIs, IMBBHs	13
2.2.3 Systematic uncertainties on standard sirens	15
2.3 Constraints on Λ CDM	16
2.3.1 H_0 tension and standard sirens	16
2.3.2 LISA forecast for H_0	17
2.3.3 Λ CDM beyond H_0	18
2.3.4 Tests of Λ CDM at high-redshift	19
2.4 Probing dark energy	20
2.4.1 Equation of state of dark energy: w_0 and w_a	20
2.4.2 Alternative dark energy models	20
2.5 Synergy with other cosmological measurements	21
2.5.1 Integration with standard electromagnetic observations	21
2.5.2 Complementarity with other gravitational wave observatories	22
2.6 Cross-correlation and interaction with large-scale structure	23
2.6.1 Cross-correlations with resolved events	23
2.6.2 Cross-correlations with the stochastic gravitational wave background	24
2.6.3 Large-scale structure effects on gravitational-wave luminosity distance estimates	26

*Section coordinator. More details at the beginning of each section.
†Document coordinator.

arXiv:2203.06016v1 [gr-qc] 11 Mar 2022

Fundamental Physics with LISA

I. Introduction	11
A. Abbreviations	13
II. Tests of General Relativity	15
A. Tests of Gravity and its fundamental principles	15
1. The Equivalence Principle	15
2. Lovelock's Theorem and GR uniqueness	15
B. Testing GR with compact objects	16
1. BHs beyond GR and theories that predict deviations	16
2. Tests with GW propagation	17
3. Tests of GR with MBH coalescence	18
4. Test of GR with EMRIs (non-null tests)	19
5. Gravitational Memory and BMS symmetry	20
C. Burning Questions and Needed Developments	21
III. Tests of the Nature of BHs	21
A. The Kerr hypothesis	21
B. Deviations from the Kerr hypothesis	22
1. BHs in non-vacuum GR	
2. ECOs: deviations from (or absence of) a classical horizon	

arXiv:2205.01597v1 [gr-qc] 3 May 2022



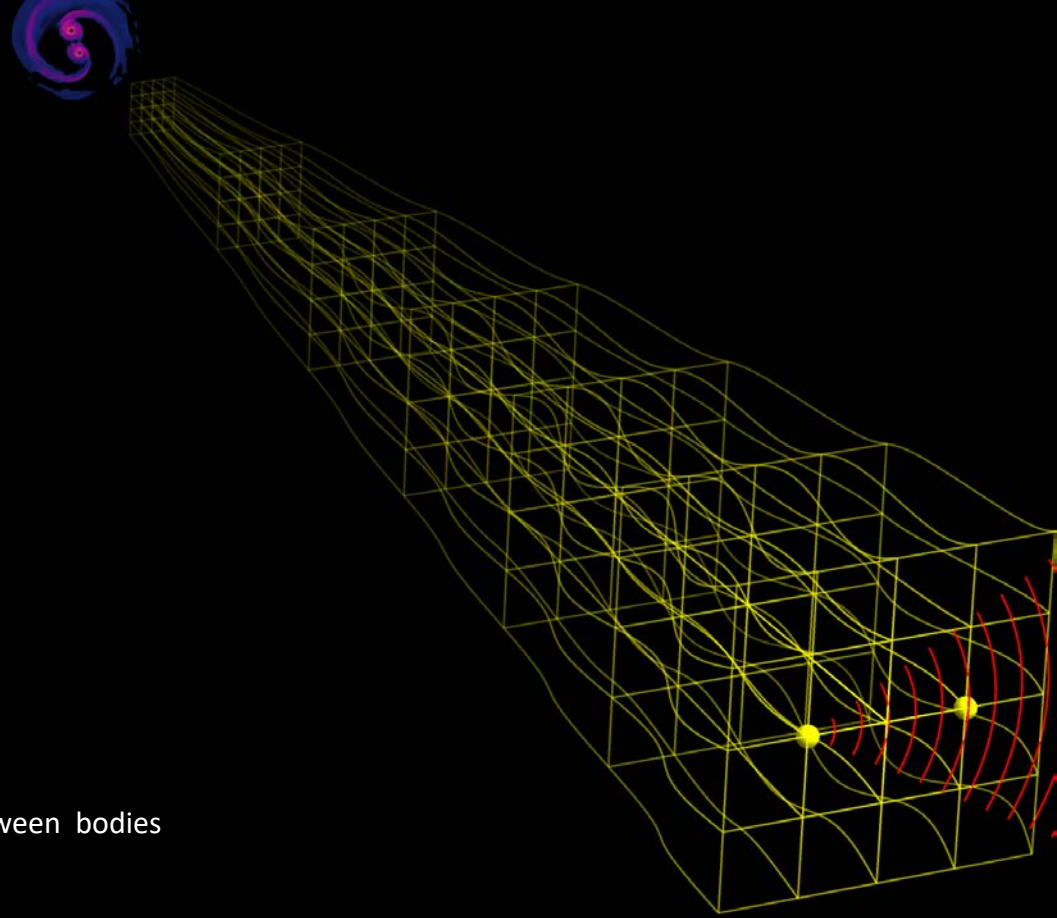
Heraklion 27/07/2022



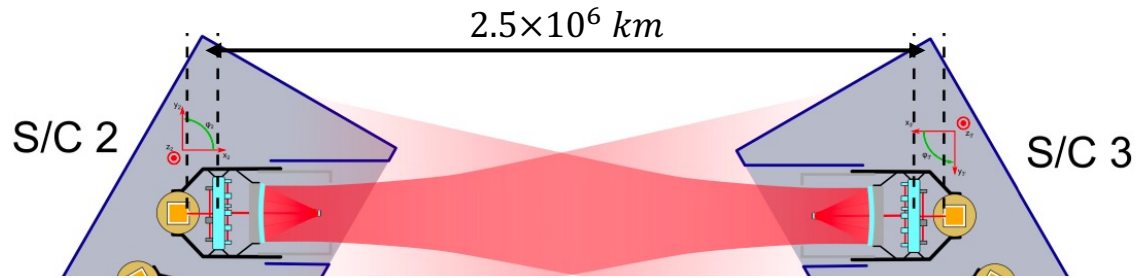
Detecting gravitational wave in space

- Waves of space-time curvature that propagate at speed of light
- Doppler tracking of free orbiting bodies modulated at period of gravitational wave

$$\frac{\Delta \dot{v}}{v_0} \approx c \underbrace{R^x_{0x0} L}_{\text{Curvature tensor}} \text{] Separation between bodies}$$



LISA



The LISA link

- Propagating throughout GW curvature, beam accumulates a time modulated frequency shift

$$\frac{\Delta \dot{\nu}}{\nu_0} \simeq \underbrace{c R^x_{0x0} L}_{\text{Curvature tensor}} \underbrace{\quad}_{\text{Size of detector}}$$



- Acceleration of spacecraft via standard Doppler effect also shifts frequency and mimics GW

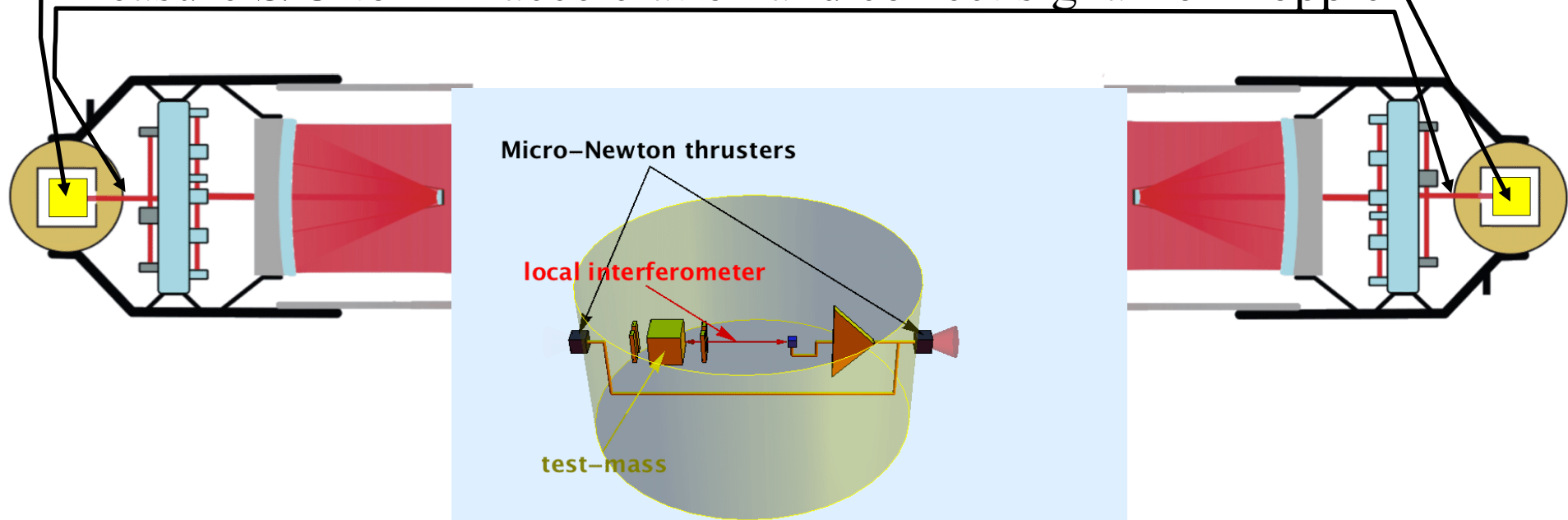
$$\frac{\Delta \dot{\nu}}{\nu_0} = c R^x_{0x0} L + \frac{a_{rec} - a_{em}}{c}$$

- Spacecraft (S/C) accelerate too much because of solar radiation pressure



Coping with S/C acceleration

- Free-floating test-masses (TM) are carried inside S/C
- No contact between TM and S/C, “drag-free” along the beam
- Measure S/C-to-TM acceleration and correct signal for Doppler



LISA link: combination of three independent measurements

2 × test-mass to spacecraft measurements

1 × spacecraft to spacecraft interferometer



$$\frac{\Delta \dot{v}_{local,1}}{v_o} = \frac{a_{TM1} - a_{SC1}}{c}$$

$$\frac{\Delta \dot{v}_{local,2}}{v_o} = \frac{a_{TM2} - a_{SC2}}{c}$$

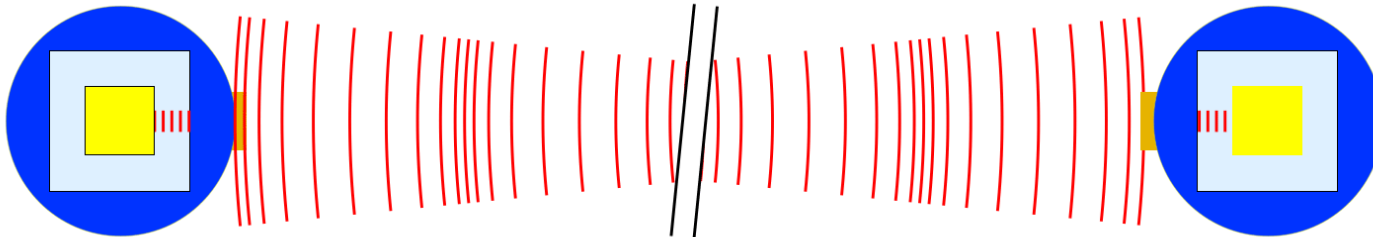
$$\frac{\Delta \dot{v}_{SC \leftrightarrow SC}}{v_o} = \frac{a_{SC2} - a_{SC1}}{c} + \frac{\Delta \dot{v}_{GW}}{v_o}$$

- Combining:

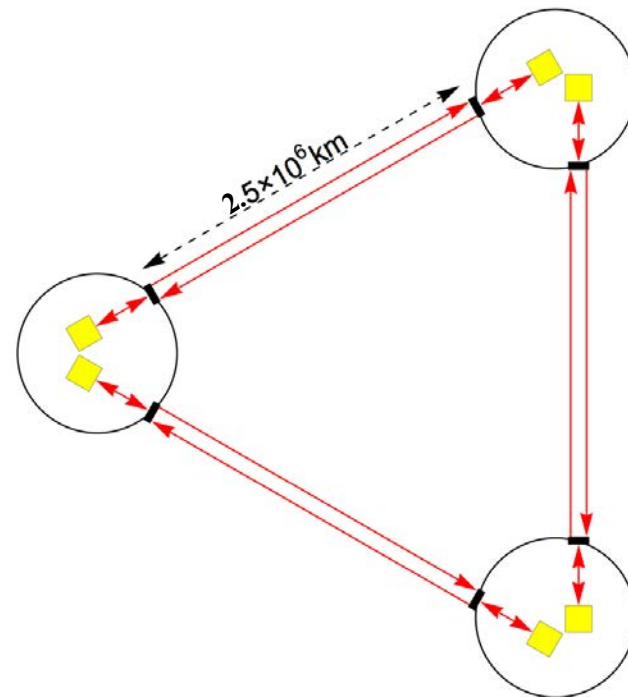
$$\begin{aligned} \frac{\Delta \dot{v}_{local,2}}{v_o} + \frac{\Delta \dot{v}_{SC \leftrightarrow SC}}{v_o} - \frac{\Delta \dot{v}_{local,1}}{v_o} &= \frac{a_{TM2} - a_{SC2} + a_{SC2} - a_{SC1} + a_{SC1} - a_{TM1}}{c} + \Delta \dot{v}_{GW} = \\ &= \frac{a_{TM2} - a_{TM1}}{c} + \Delta \dot{v}_{GW} \end{aligned}$$

Equivalent to a direct test-mass to test-mass measurement

The LISA arm

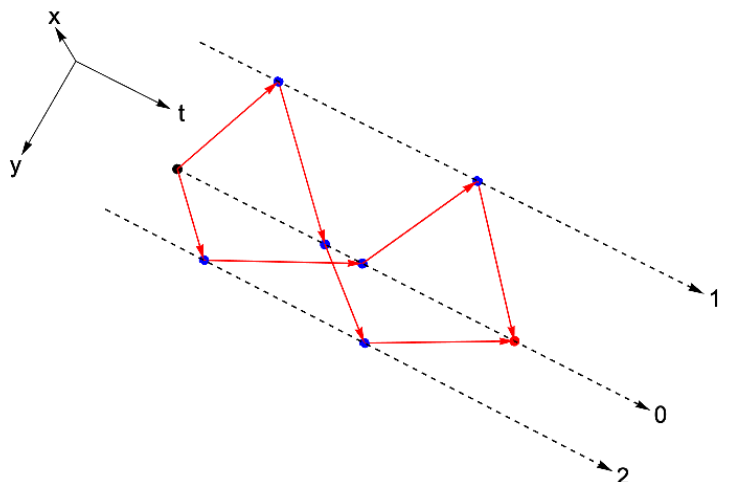
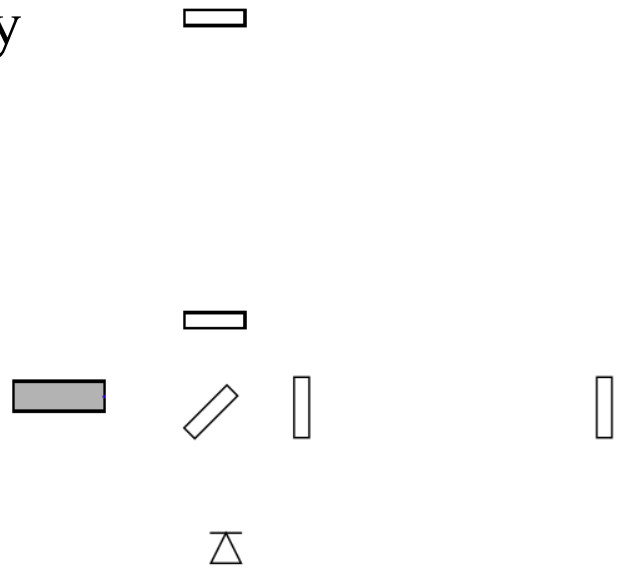


- True reflection impossible. The LISA arm: two counter-propagating links.
- LISA: 3 arms=6 links
- LISA science signals: 1 frequency signal per link, i.e. 6 single-link signals

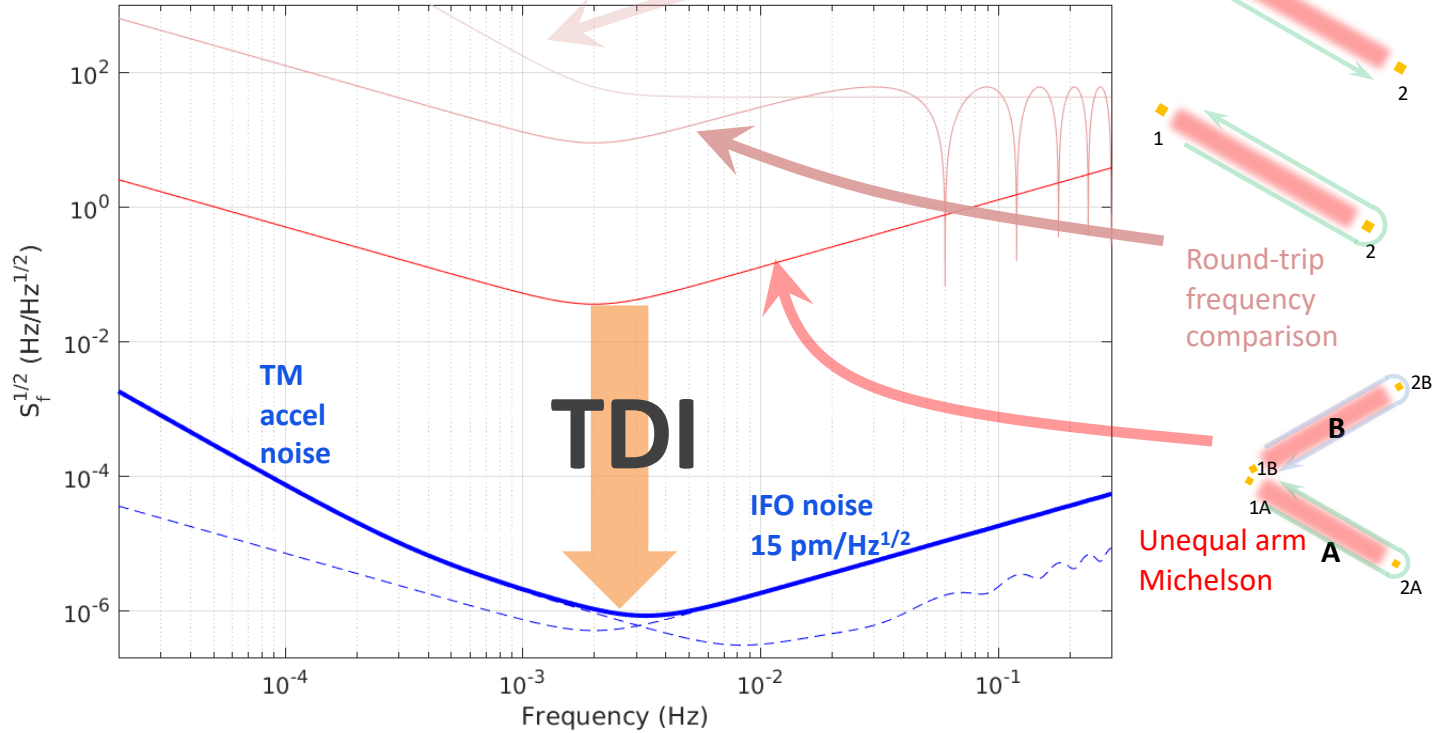


Laser frequency noise & time delay interferometry

- Best stabilized laser frequency noise off scale:
 - Required $\leq 1 \mu\text{Hz}/\sqrt{\text{Hz}}$
 - Available $\leq 1 \text{kHz}/\sqrt{\text{Hz}}$
- Ground based interferometers beat noise comparing beams emitted at same time (equal arms)
- LISA: arms are unequal ($\Delta L \simeq 10^5 \text{km}$) and time varying over the year.
- Combine single-link signals to mimic light beams that have traveled equal lengths



8 orders of magnitude suppression



Requires high accuracy measurement of phase

- Demonstrated in lab by many teams
- For instance

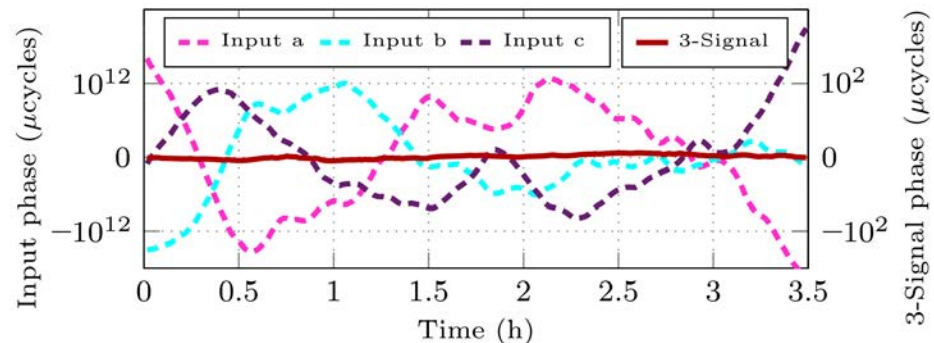
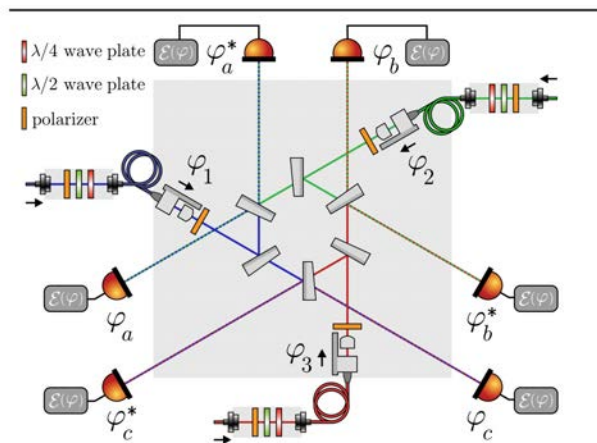


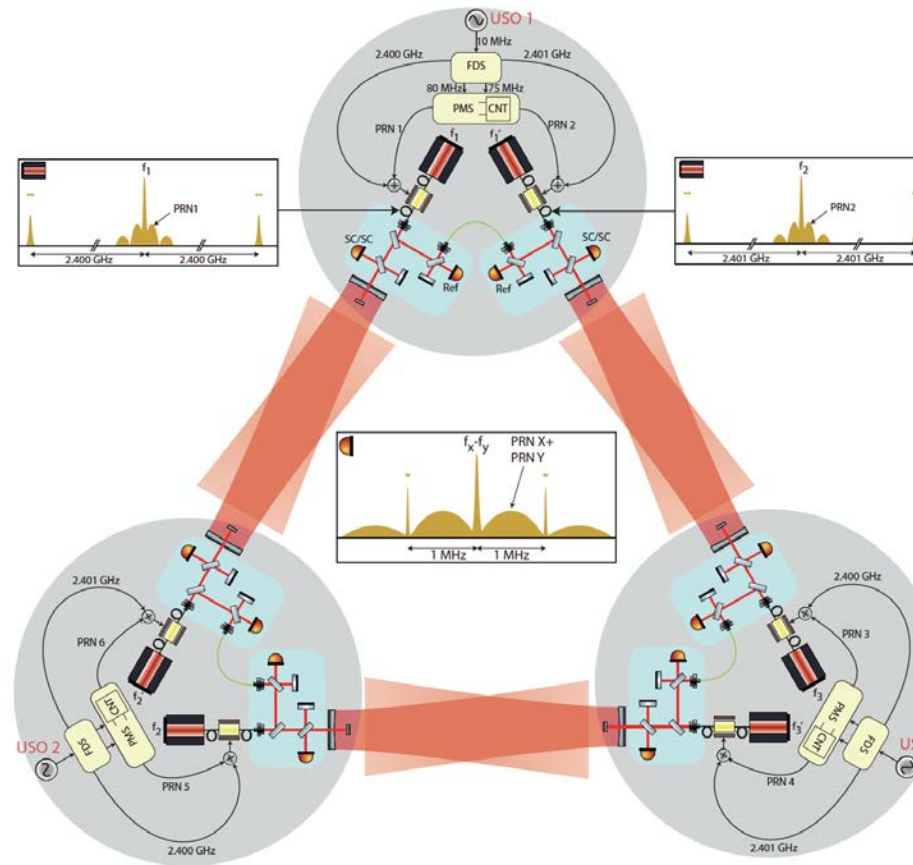
FIG. 4. Time series of input phase fluctuations and resulting three-signal combination, illustrating the high dynamic range essential for TDI.

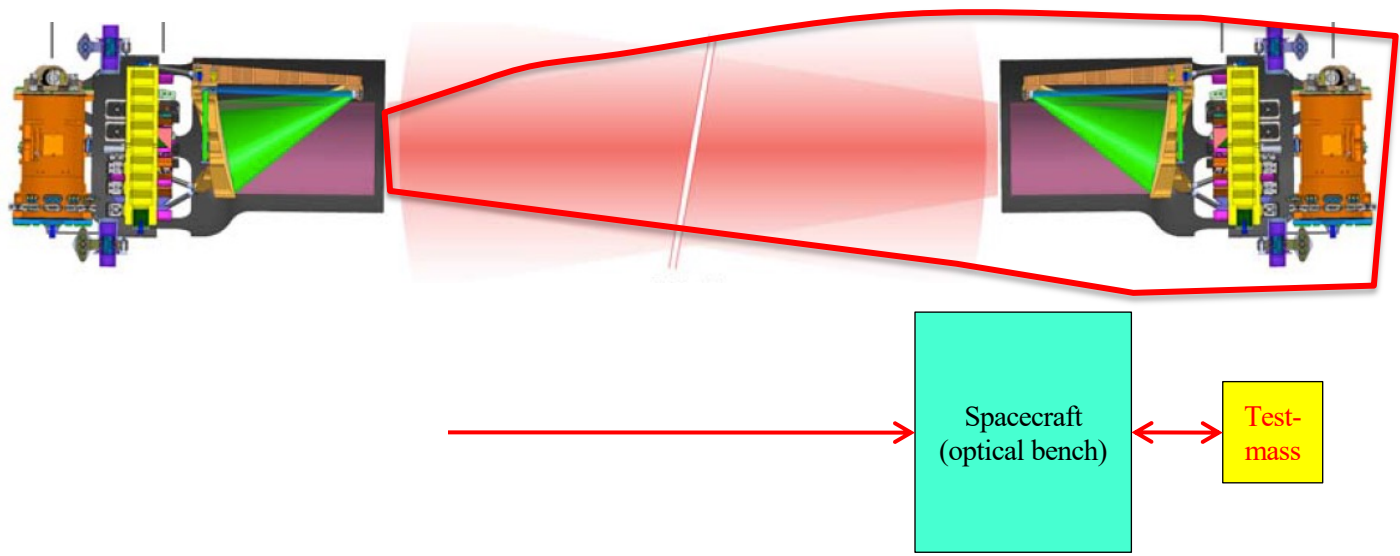
$10^8 - 10^{11}$ dynamic range

PHYSICAL REVIEW LETTERS **122**, 081104 (2019)

Time delay interferometry

- Requires knowledge of light travel time within 3 ns/1 m
- Done with “laser GPS”:
 - Pseudo-random code transmitted as modulation of laser frequency
 - Received signal correlated locally with same code to find true delay
- Predicted accuracy 1 – 10 cm

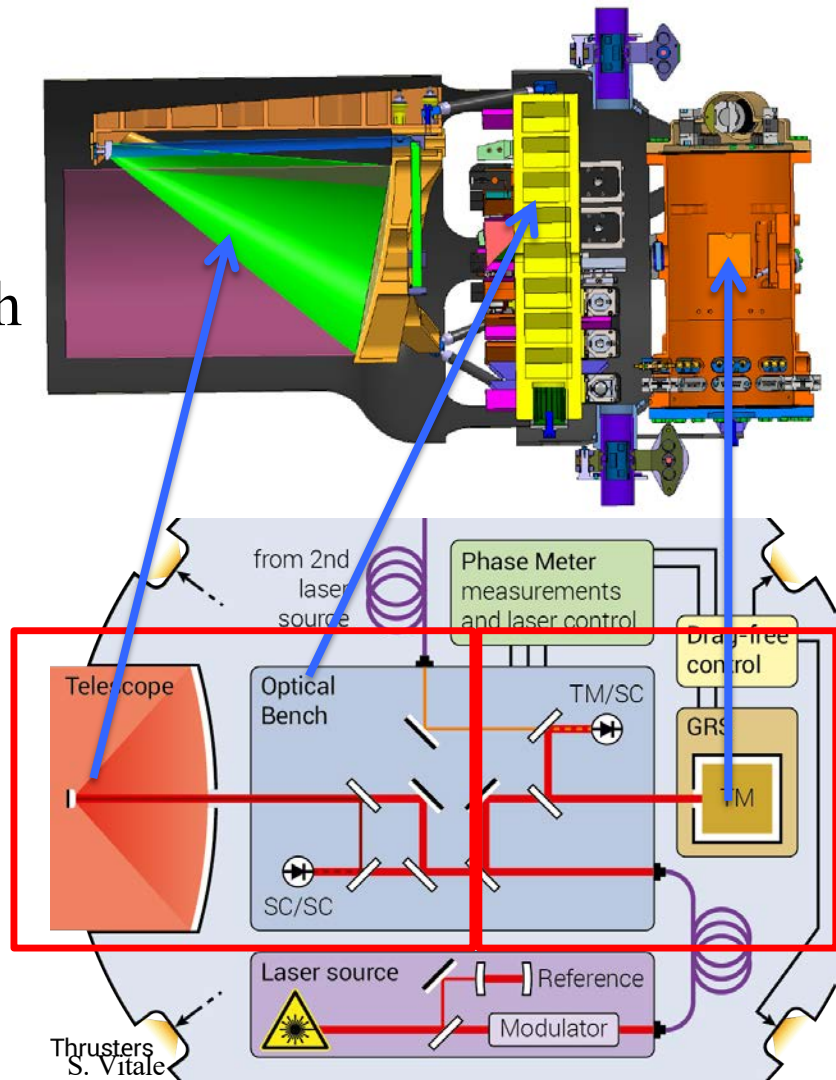




The LISA link instrument

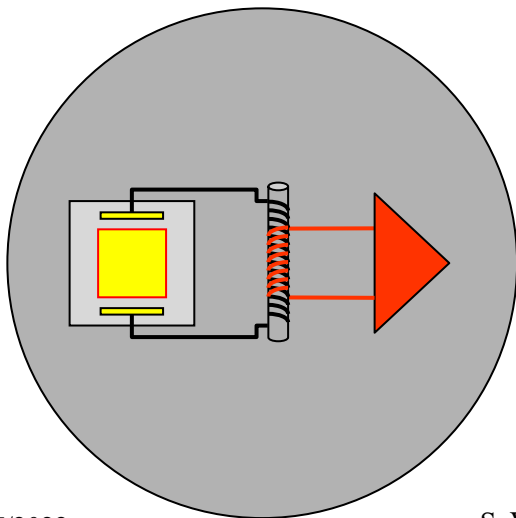
LISA link Instrument

- The Gravitational Reference Sensor with the test-mass
- The Optical Bench with:
 - Local interferometer
 - Spacecraft to spacecraft interferometer, including telescope

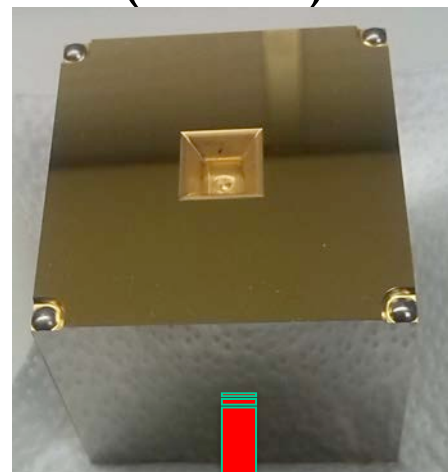


The Gravity reference Sensor (GRS)

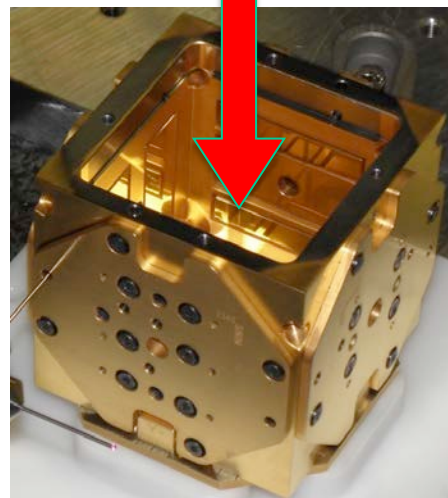
- Drag-free along sensitive direction
- Other test-mass degrees of freedom controlled via electrostatic forces
- 3-4 mm clearance between test-mass and electrodes



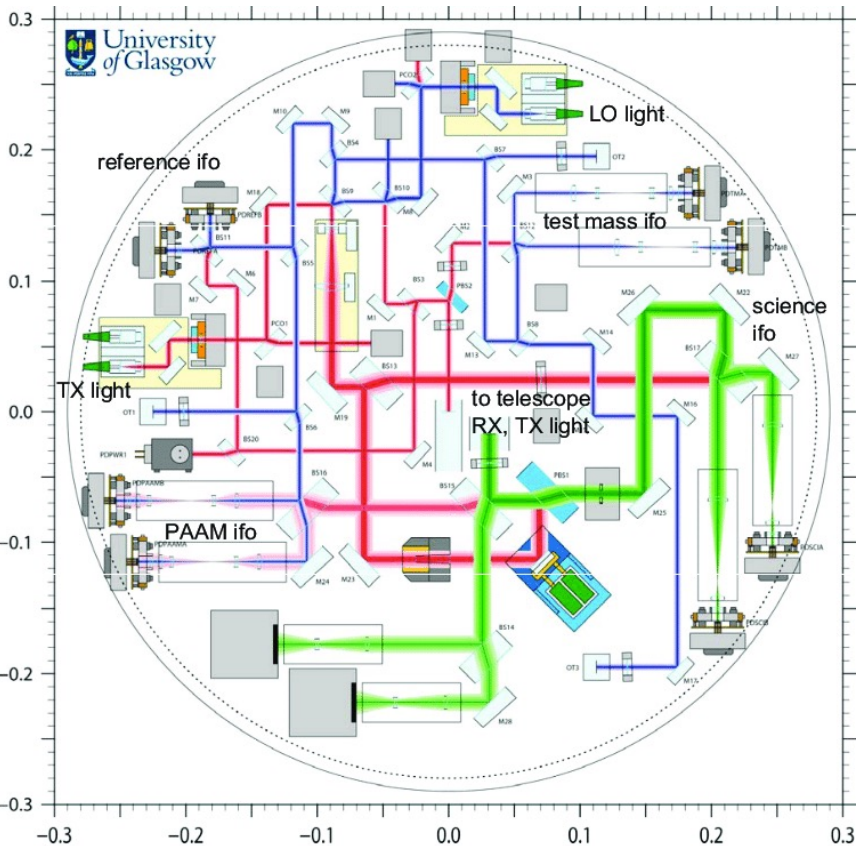
test-mass



electrode housing



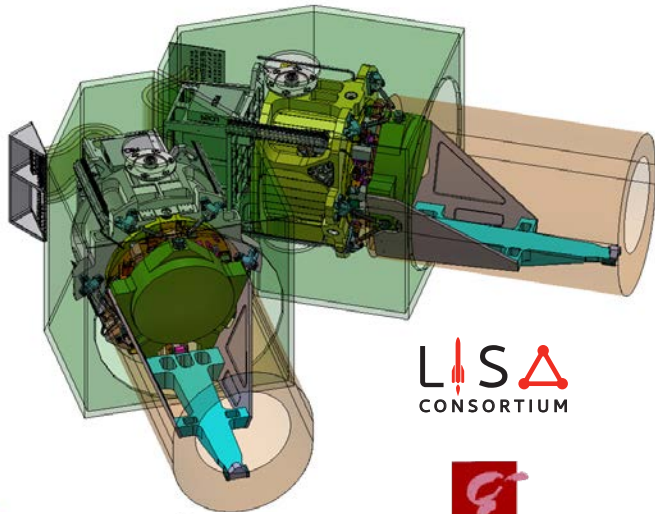
The optical bench



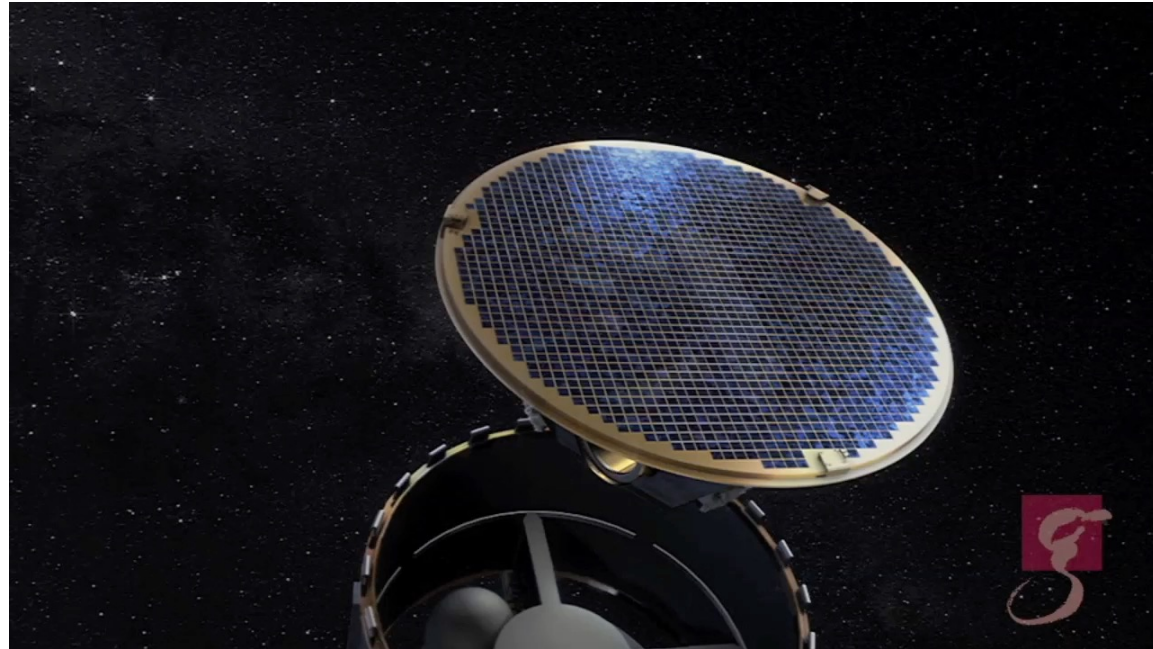
21



The full complement

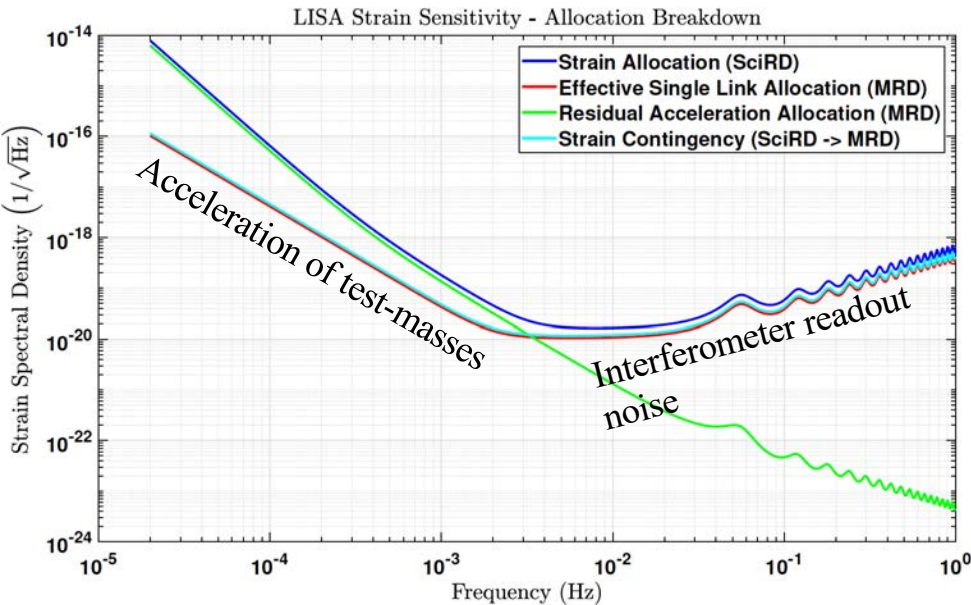


LISA
CONSORTIUM



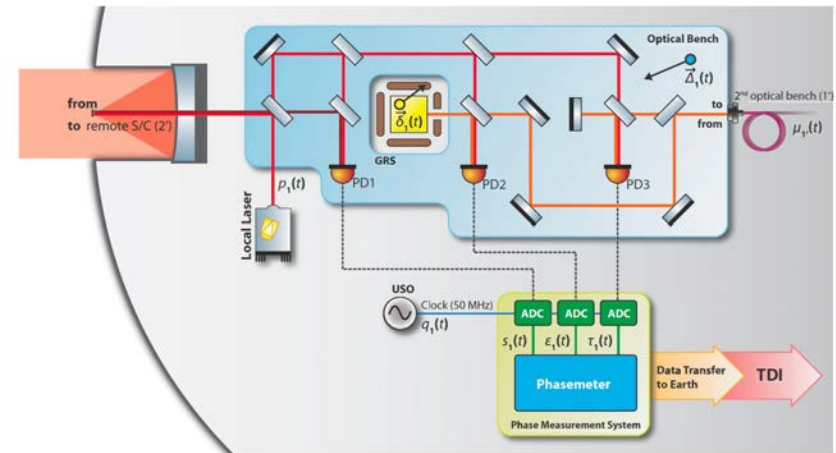
Noise in a LISA link

- Once frequency noise has been suppressed, LISA sensitivity limited at low frequency by acceleration of test-masses
- Only at higher frequencies interferometer readout noise sets in

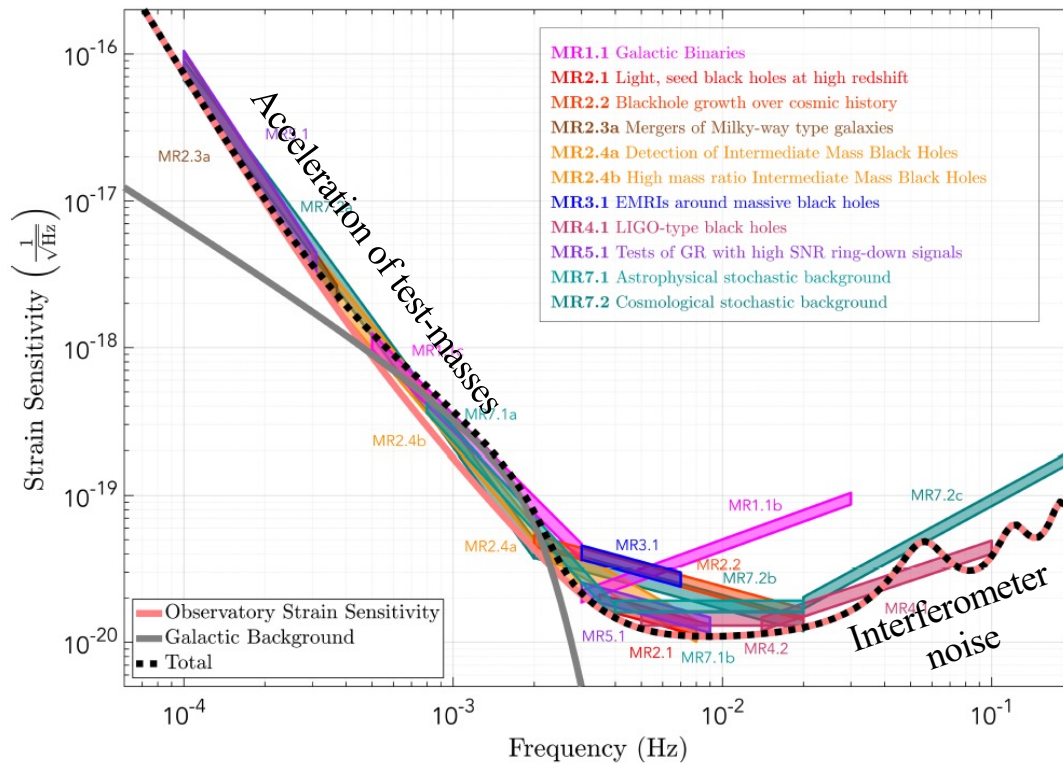


Class. Quantum Grav. **29** (2012) 205003

M Otto *et al*

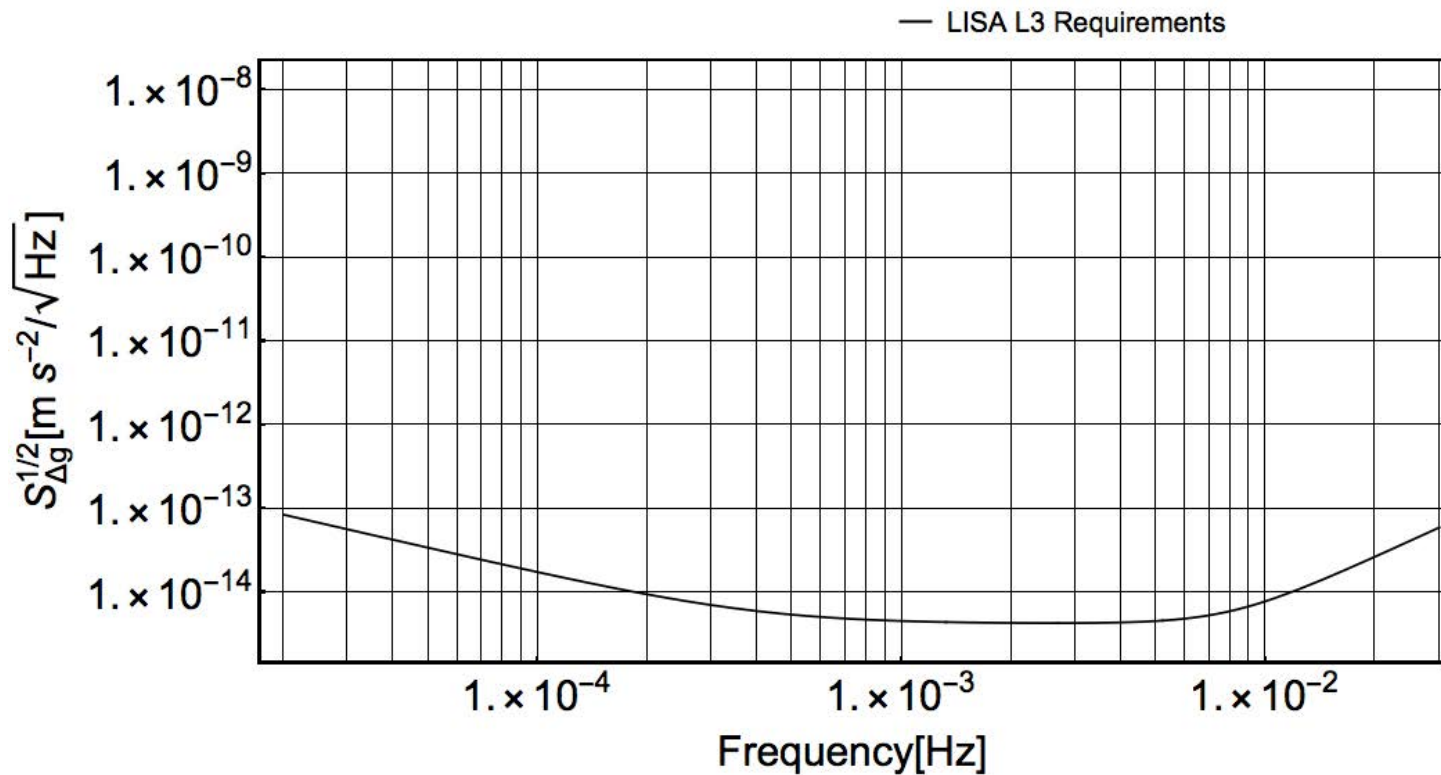


- LISA sensitivity limited at low frequency by acceleration of test-masses
- LISA is a low frequency instrument: much of SNR for most interesting sources accumulated $\lesssim 10$ mHz



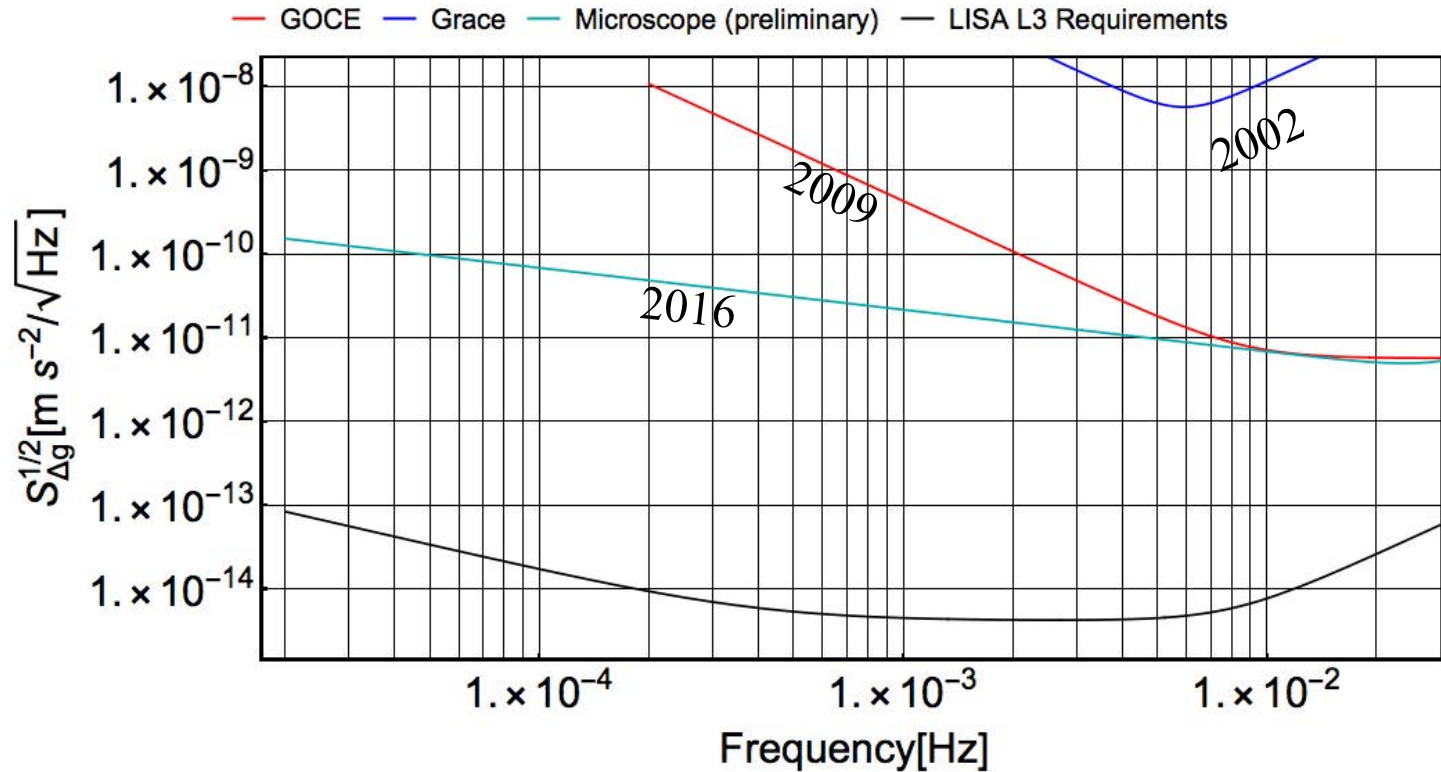
LISA: Sub-femto-g force suppression required

- Cannot be tested on ground \approx 0.1 Hz



LISA: Sub-femto-g force suppression required

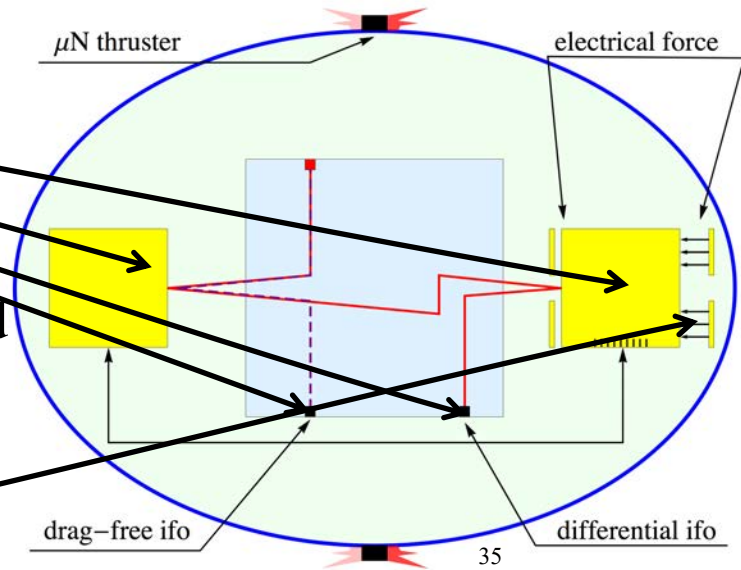
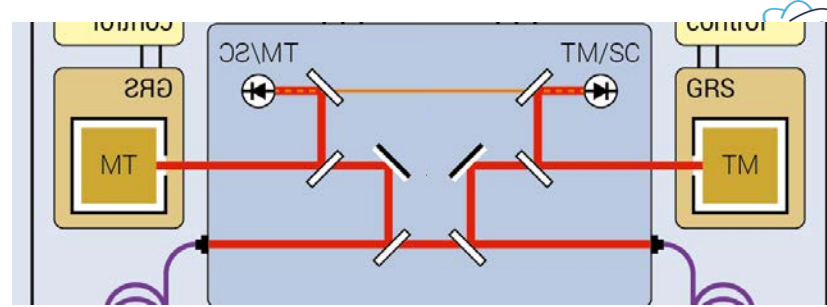
- Cannot be tested on ground ≈ 0.1 Hz
- Not even in low Earth orbit: orders (>3) of magnitude better than any other space mission





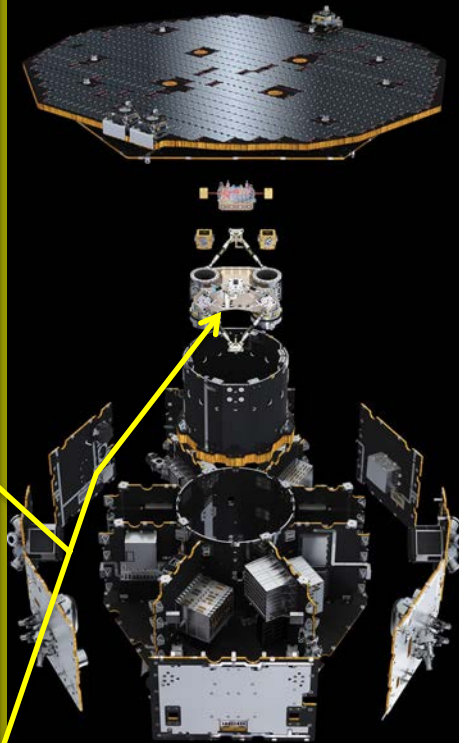
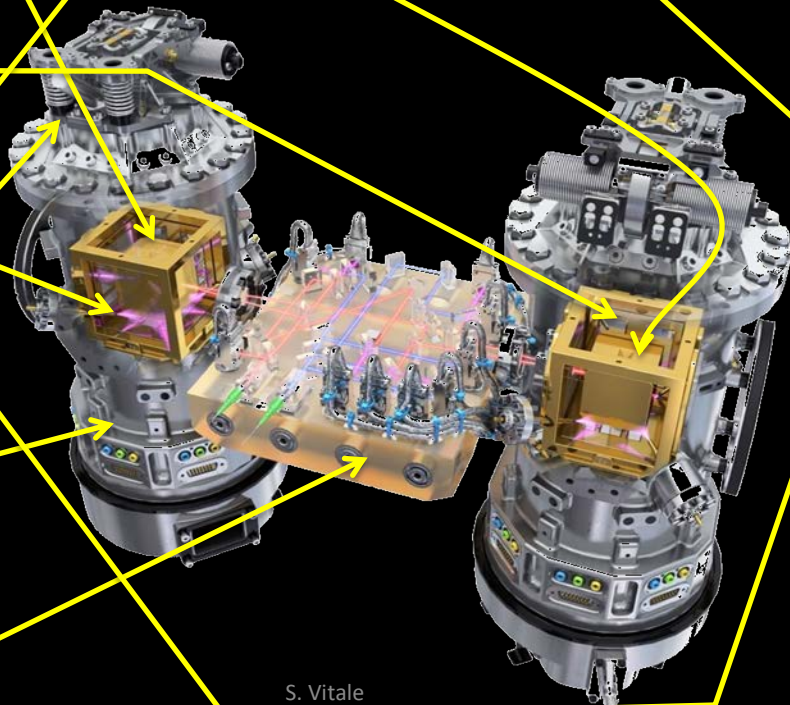
LISA Pathfinder

- Force disturbance is local. Test does not require million km size
- One LISA link inside a single spacecraft (no million km arm)
- 2 TMs,
- 2 Interferometers (Ifo)
- Satellite chases one test-mass
- Contrary to LISA, second test-mass forced to follow the first at very low frequency by electrostatics

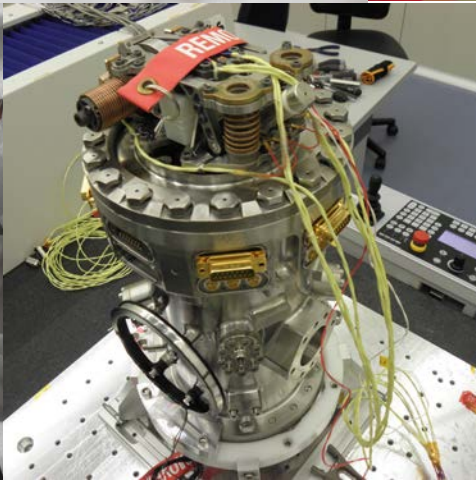
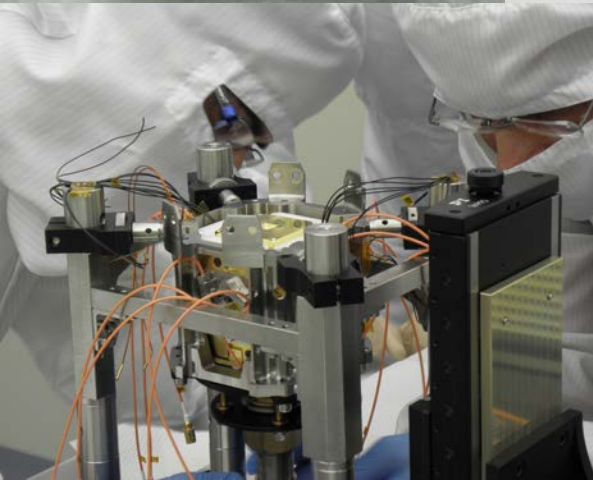
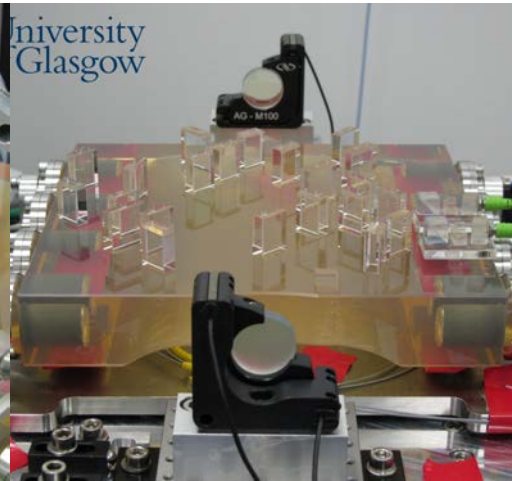
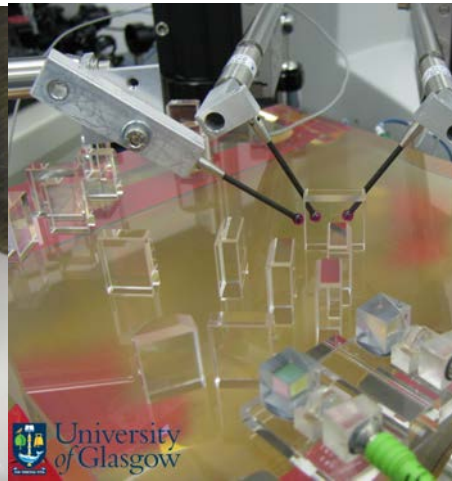
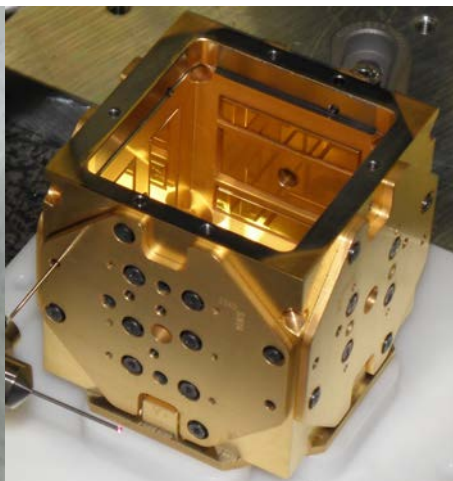
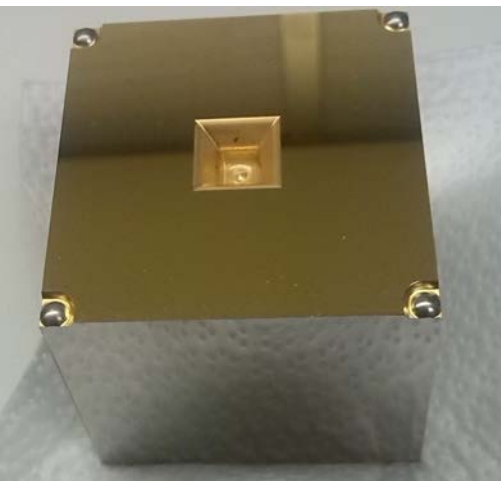


The LTP

- Test masses gold-platinum, highly non-magnetic, very dense
- Electrode housing: electrodes are used to exert very weak electrostatic force
- UV light, neutralize the charging due to cosmic rays
- Caging mechanism: holds the test-masses and avoid them damaging the satellite at launch
- Vacuum enclosure to handle vacuum on ground
- Ultra high mechanical stability optical bench for the laser interferometer

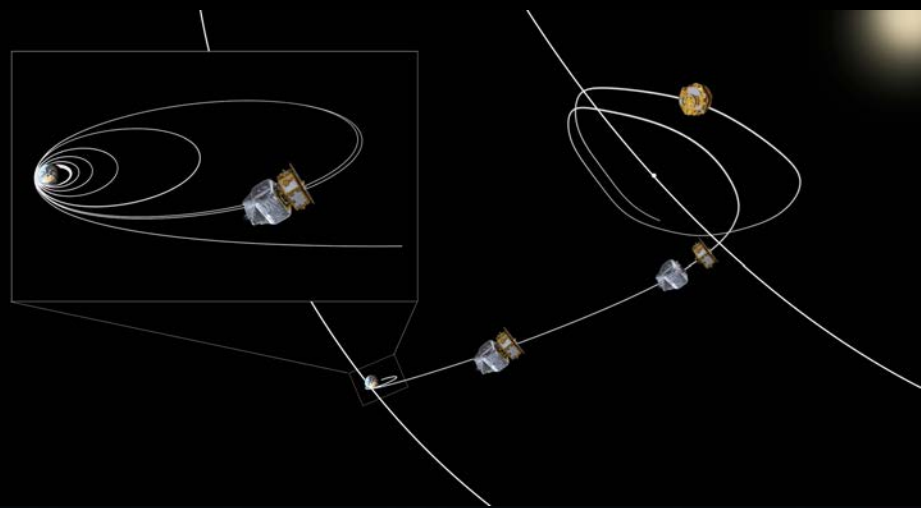
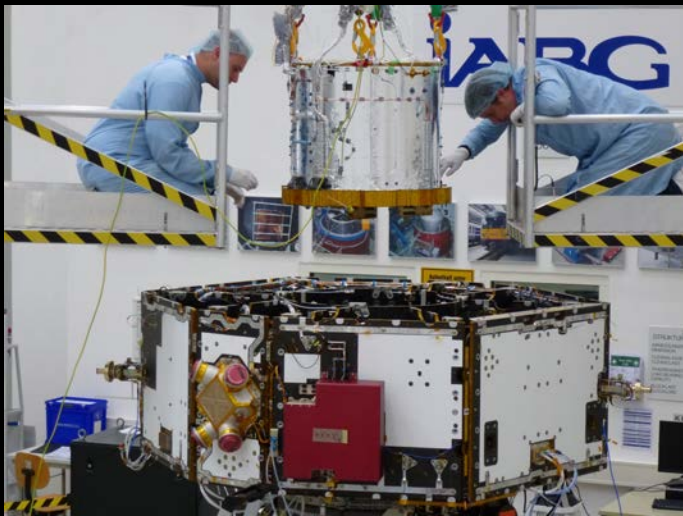


The real H/W



Instrument integration





From instrument integration to orbit





1 Mar – 27 June
Science operations

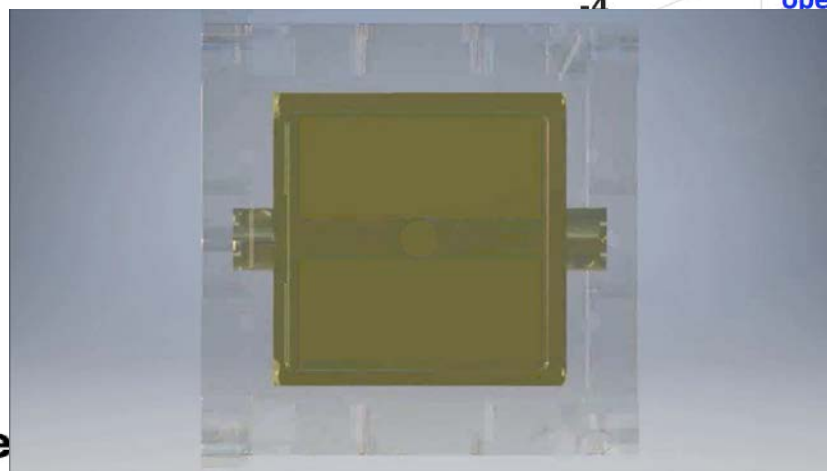
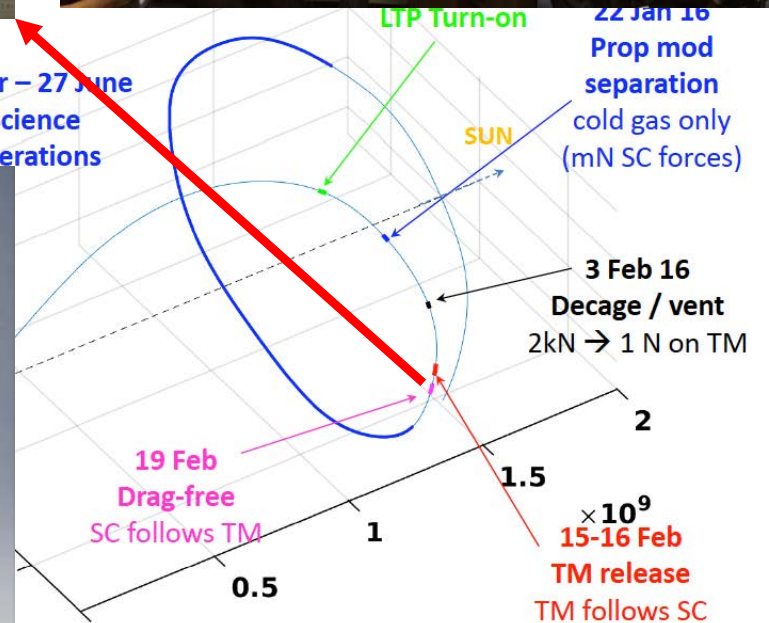
LTP Turn-on

22 Jan 16
Prop mod separation
cold gas only
(mN SC forces)

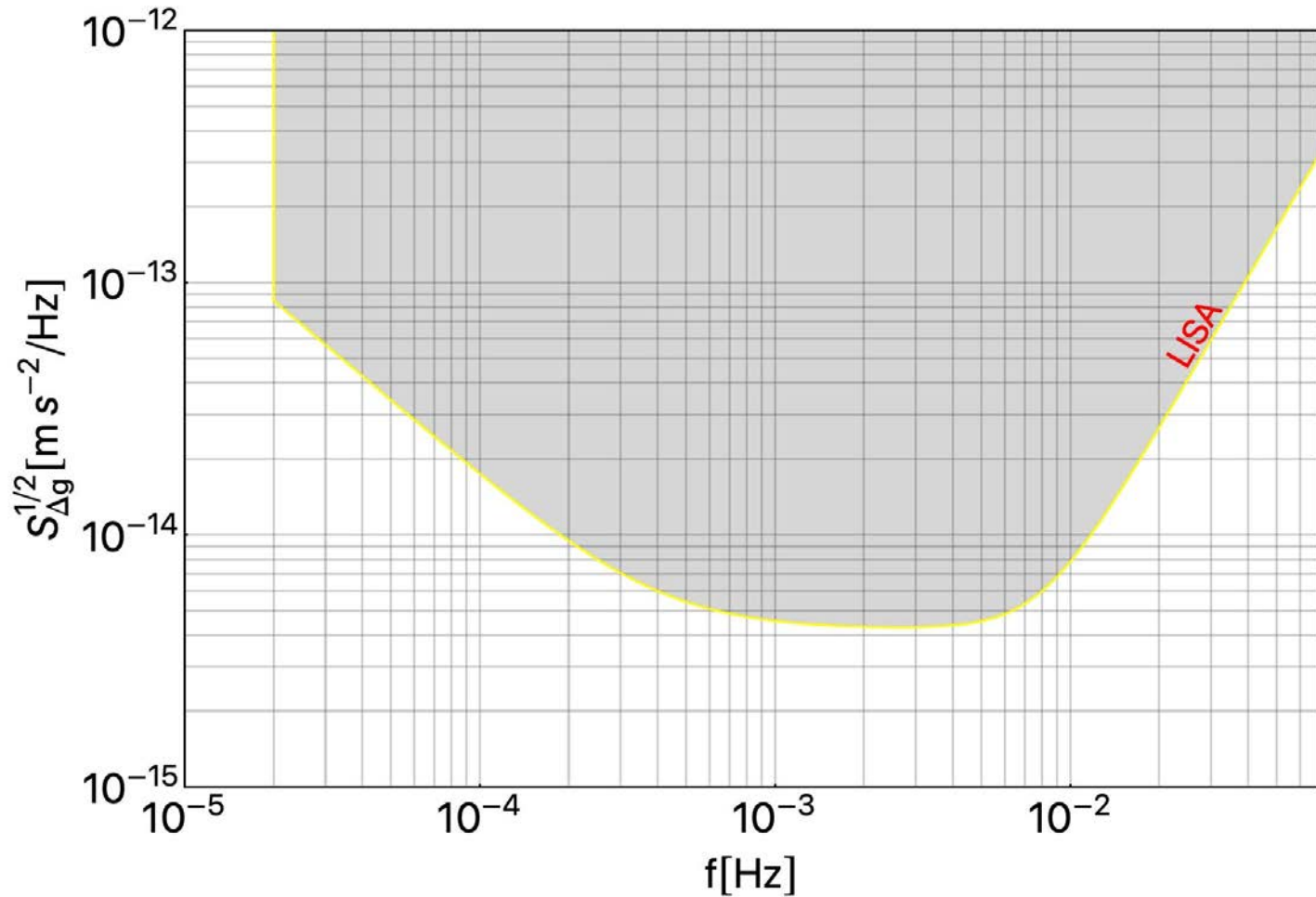
3 Feb 16
Decage / vent
2kN → 1 N on TM

19 Feb
Drag-free
SC follows TM

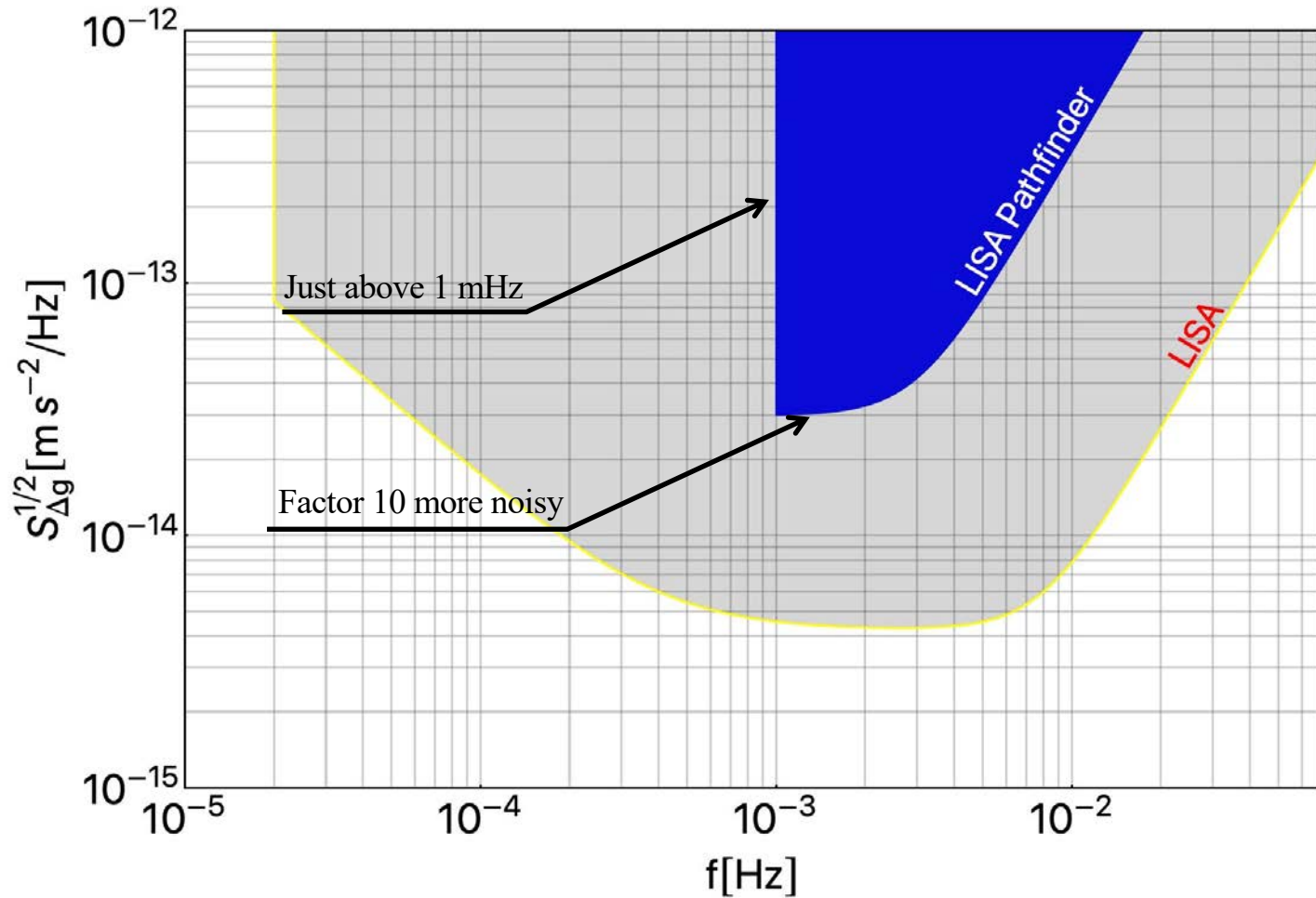
15-16 Feb
TM release
TM follows SC



LISA acceleration requirements



Relaxed LISA Pathfinder requirements



Expected performance

- LISA Pathfinder performance budget: 276pages
- A short list of dominating effects

Airbus	Experiment Performance Budget	LTP
LTP Equipment Parameters		
	OMS Parameters	144
	ISS Parameters	147
	Derived Parameters	151
LPF System Parameters (ASU)		
	System Fields	153
	DFACS Performance	155
B2 - DC Differential Forces and Absolute Torques		
	Differential X-Force [DCX]	158
	Electric Field [DCX1000]	158
	Magnetic Field [DCX2000] (ASU)	158
	Thermal Effects [DCX3000]	158
	Radiometer Effect [DCX3100]	158
	Differential Radiation Pressure [DCX3200]	158
	Laser [DCX4000]	159
	Gravitational Field [DCX5000] (ASU)	159
	Margin [MDCX]	159
	Differential Y-Force [DCY]	159
	Electric Field [DCY1000]	159
	Magnetic Field [DCY2000] (ASU)	160
	Thermal Effects [DCY3000]	160
	Radiometer Effect [DCY3100]	160
	Differential Radiation Pressure [DCY3200]	160
	Gravitational Field [DCY4000] (ASU)	160
	Margin [MDCY]	161
	Differential Z-Force [DCZ]	161
	Electric Field [DCZ1000]	161
	Magnetic Field [DCZ2000] (ASU)	161
	Thermal Effects [DCZ3000]	161
	Radiometer Effect [DCZ3100]	161
	Differential Radiation Pressure [DCZ3200]	162
	Gravitational Field [DCZ4000] (ASU)	162
	Margin [MDCZ]	162
	Absolute ϕ -Torque [DC ϕ]	162
	Electric Field [DC ϕ 1000]	162
	Magnetic Field [DC ϕ 2000] (ASU)	162
	Thermal Effects [DC ϕ 3000]	163
	Radiometer Effect [DC ϕ 3100]	163
	Differential Radiation Pressure [DC ϕ 3200]	163
	Gravitational Field [DC ϕ 4000] (ASU)	163

Airbus	Experiment Performance Budget	LTP
	Margin [MDC ϕ]	163
	Absolute η -Torque [DC η]	164
	Electric Field [DC η 1000]	164
	Magnetic Field [DC η 2000] (ASU)	164
	Thermal Effects [DC η 3000]	164
	Radiometer Effect [DC η 3100]	164
	Differential Radiation Pressure [DC η 3200]	164
	Gravitational Field [DC η 4000] (ASU)	165
	Margin [MDC η]	165
	Absolute ϕ -Torque [DC ϕ]	165
	Electric Field [DC ϕ 1000]	165
	Magnetic Field [DC ϕ 2000] (ASU)	165
	Thermal Effects [DC ϕ 3000]	165
	Radiometer Effect [DC ϕ 3100]	165
	Differential Radiation Pressure [DC ϕ 3200]	166
	Gravitational Field [DC ϕ 4000] (ASU)	166
	Margin [MDC ϕ]	166
B3 - Differential Acceleration Noise in the MBW		
	Direct Forces [R10000]	167
	Internal Forces [R11000]	167
	Readout Back-action [R11100]	167
	Thermal Effects Within Sensor [R11200]	167
	Brownian Noise Terms [R11300]	169
	Magnetic Field Effects [R11400] (ASU)	170
	Random Charging and Voltage Effects [R11500]	171
	Laser Radiation Pressure [R11600]	171
	Self Gravity Noise [R11700]	171
	Stray-Voltage Fluctuation within MBW [R11800]	172
	AC voltage down-conversion [R11900]	172
	Margin [M11000]	172
	Sensitive Axis Electrostatic Actuation [R12000]	172
	Multiplicative noise in MBW coupling via AC actuation voltages [R12100]	172
	Down conversion of additive voltage noise at AC actuation frequency (around 100Hz) [R12200]	173
	Coupling of additive voltage noise in measurement bandwidth with DC voltage and DC charge [R12300]	173
	Down conversion of additive voltage noise at AC injection frequency (100kHz) [R12400]	173
	Margin [M12000]	175
	Cross-Axes Coupling [R13000]	175

Class. Quantum Grav. 28 (2011) 094002

F Antonucci *et al*

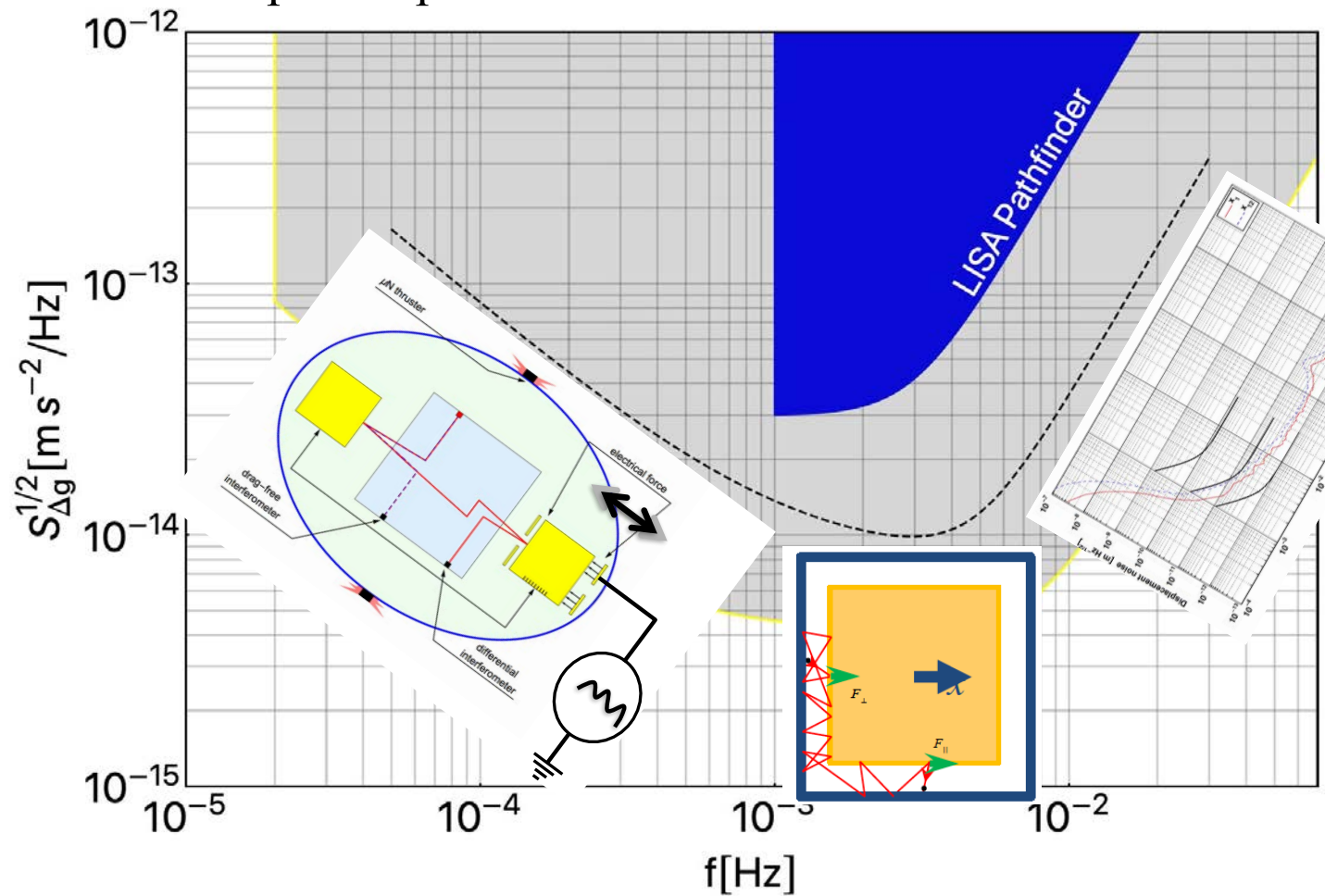
Table 2. Leading sources of differential force-per-unit-mass disturbances and their PSD values at 1 mHz.

Source	PSD (fm s ⁻² Hz ^{-1/2})	Estimated from
Actuation, x-axis	7.5 (0.8) ^a	Measurement of flight-model electronics stability
Brownian	7.2	Measurement with torsion pendulum
Magnetics	2.8	Measurement of magnetic field stability
Stray voltages	1.1	Upper limit from the torsion pendulum test campaign
Laser radiation pressure	0.7	Measurement of laser power stability
Force from dynamics of other DoF	0.4	From simulated dynamics of DoF other than x , and estimated worst-case values of $\overleftrightarrow{\delta D}$ and $\overleftrightarrow{\delta C}$
Thermal gradient effects	0.4	Upper limit from the torsion pendulum test campaign
Self-gravity noise	0.3	Upper limit from thermo-elastic stability simulations
Noisy charge	0.1	Upper limit from the charge simulation and measured voltage balance
Coupling to SC motion via force gradients	0.1	From the estimation of stiffness and simulated SC jitter
Total	10.9 (7.9) ^a	Root square sum

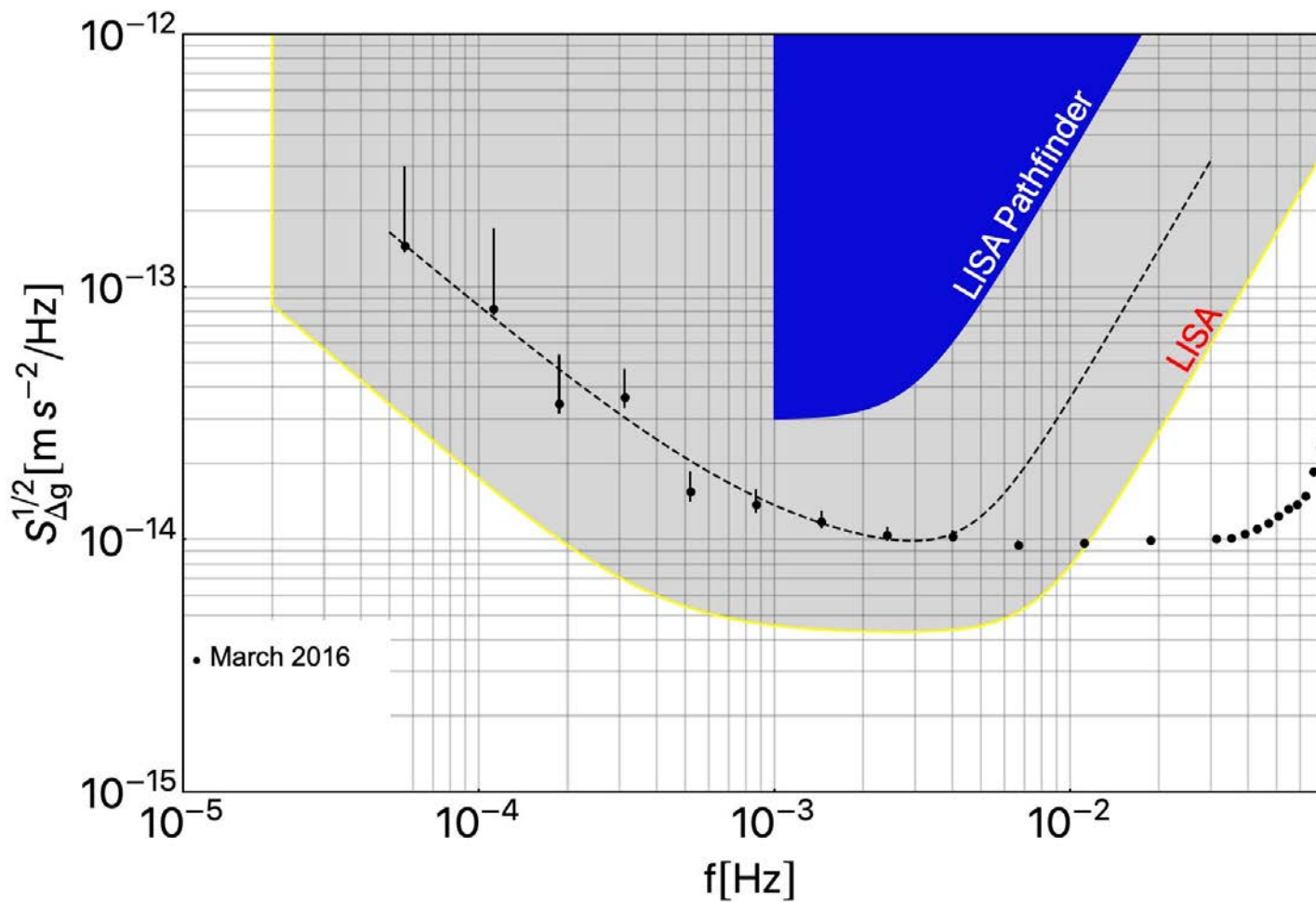
^a The values within parentheses refer to the free-flight mode. See the text for explanation.

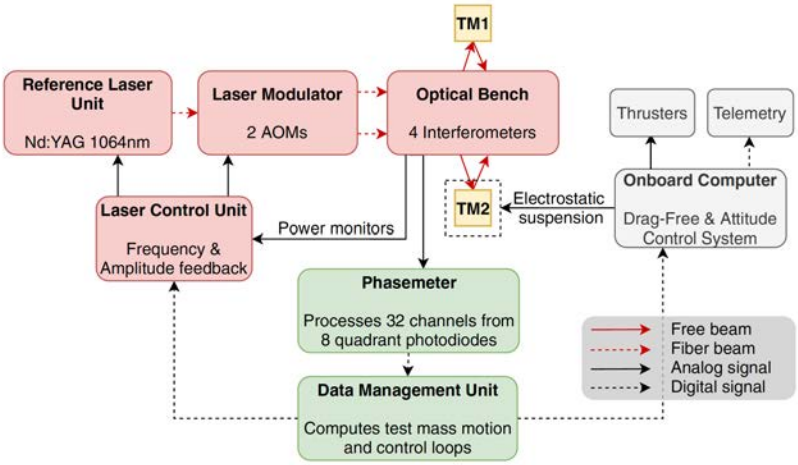
Expected performance

- Electrostatic actuation noise:
 - For a given voltage source noise, the larger the needed force you set, the larger the force noise.
- Brownian noise from residual gas:
 - The larger the pressure surrounding the test-mass the larger the noise
- Interferometer readout noise: $\approx 10 \text{ pm}/\sqrt{\text{Hz}}$ as for LISA



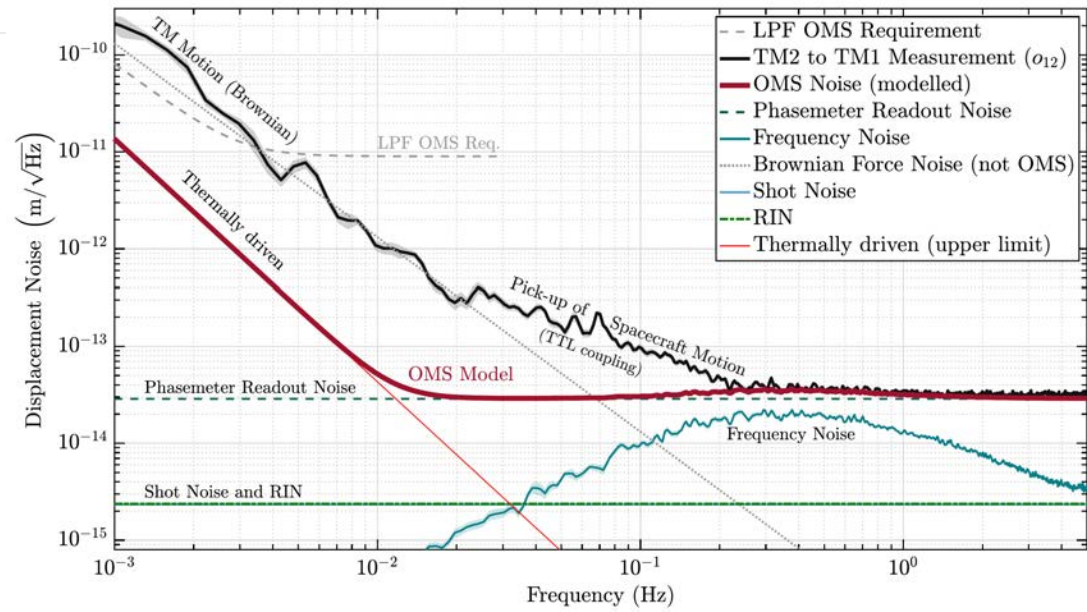
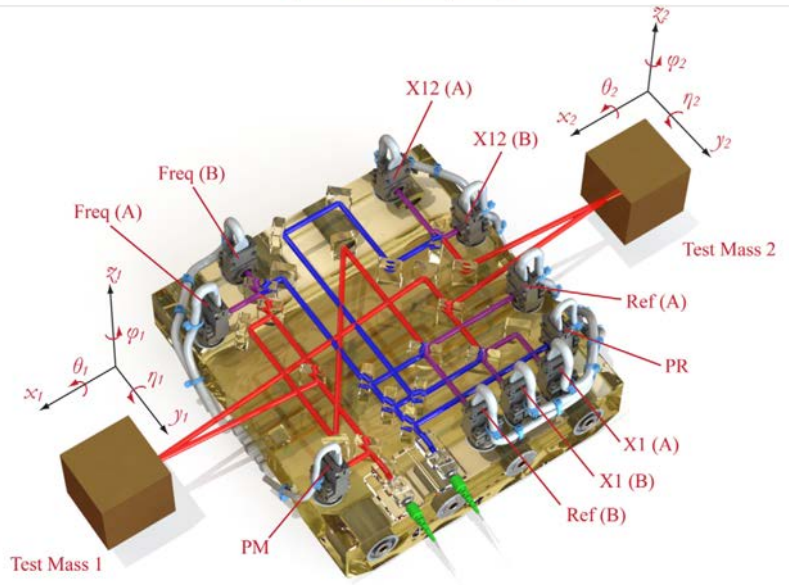
- Better than requirement.
- Close to prediction
- Except for interferometer noise at 35 fm/√Hz instead of 10 pm/√Hz





The magic interferometer

PHYSICAL REVIEW LETTERS 126, 131103 (2021)



Gravitational control and actuation

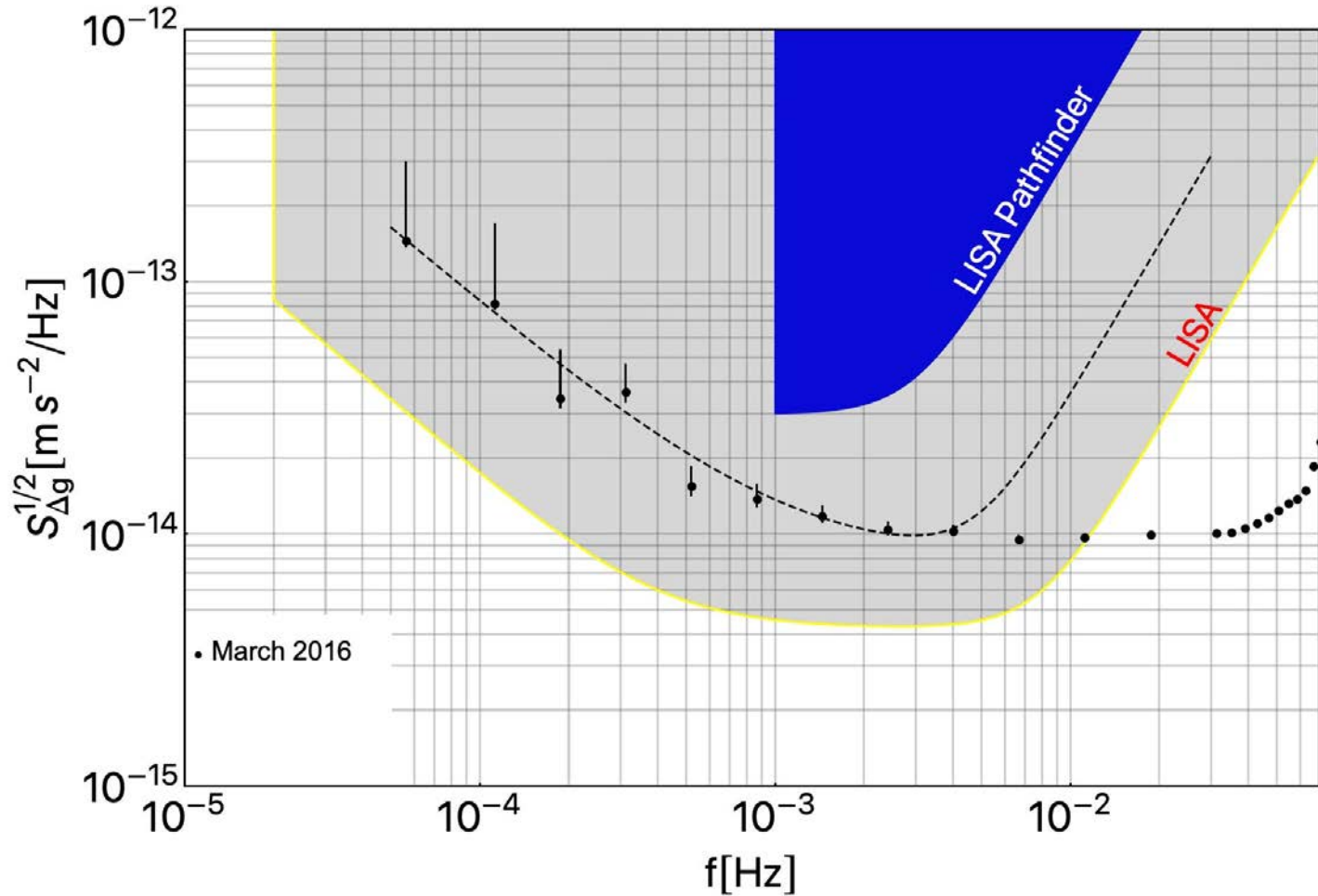
- Electrostatic force mostly compensates gravitational force
- Gravitational force canceled in dead reckoning with ~ 1.8 kg balance mass
- Specification $g_{\max} < 650 \text{ pm s}^{-2}$ ($3 \sigma + \text{margin}$)

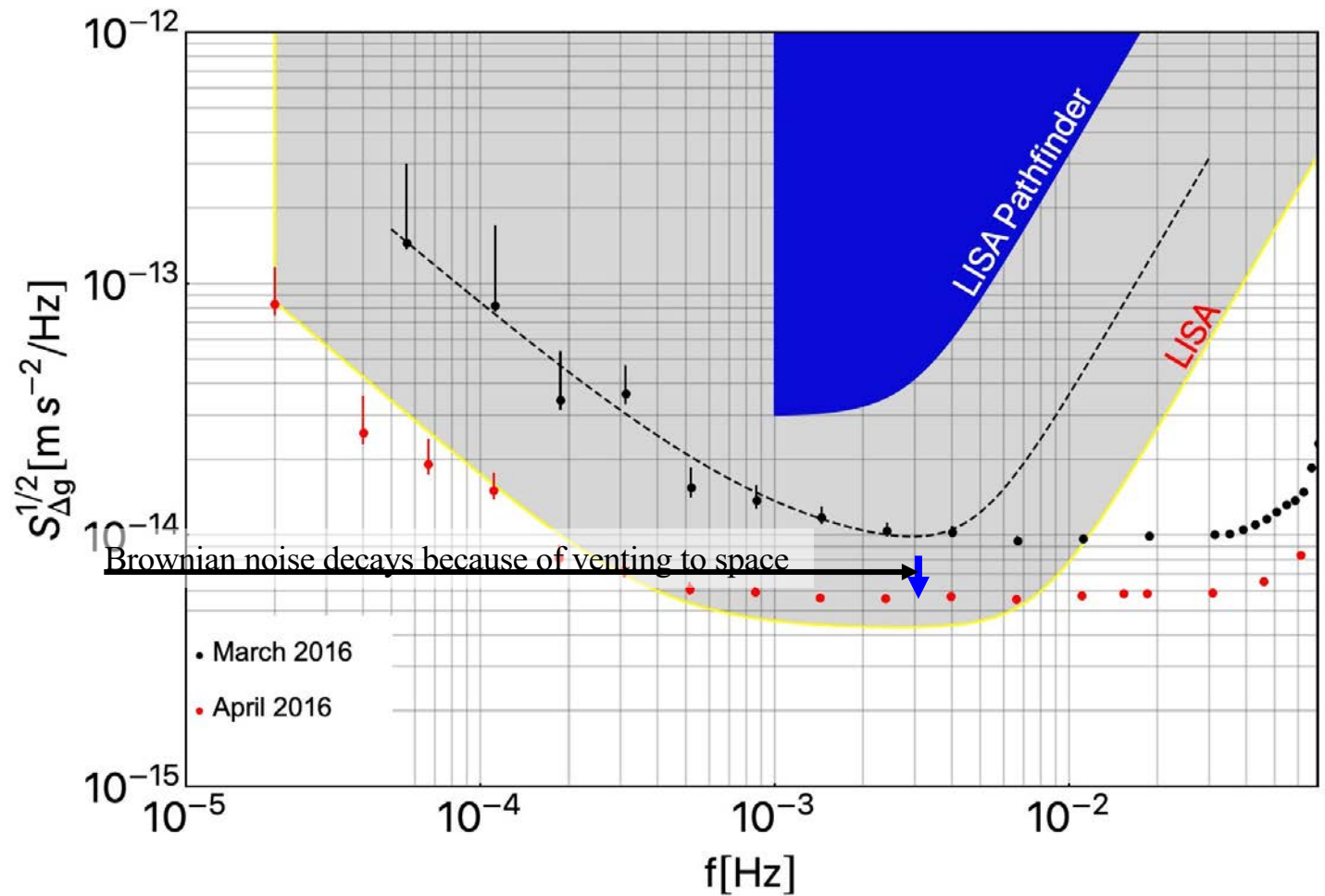
EADS LISA Pathfinder
AVX Mass Tracking Log
Page No. 3/4

Line No.	Date	Type	ATS Reference	Description of Mass Adjustment (see Remarks Column)	Description of Location	Item Name	Part No.	Quantity	Temp. (K)	Temp. (C)	In Model
1001	2011-07-27	Cal	AVX-001	Initial calibration	AVX-001	AVX-001	AVX-001	1	293.15	20.0	Y
1002	2011-07-27	Cal	AVX-002	Initial calibration	AVX-002	AVX-002	AVX-002	1	293.15	20.0	Y
1003	2011-07-27	Cal	AVX-003	Initial calibration	AVX-003	AVX-003	AVX-003	1	293.15	20.0	Y
1004	2011-07-27	Cal	AVX-004	Initial calibration	AVX-004	AVX-004	AVX-004	1	293.15	20.0	Y
1005	2011-07-27	Cal	AVX-005	Initial calibration	AVX-005	AVX-005	AVX-005	1	293.15	20.0	Y
1006	2011-07-27	Cal	AVX-006	Initial calibration	AVX-006	AVX-006	AVX-006	1	293.15	20.0	Y
1007	2011-07-27	Cal	AVX-007	Initial calibration	AVX-007	AVX-007	AVX-007	1	293.15	20.0	Y
1008	2011-07-27	Cal	AVX-008	Initial calibration	AVX-008	AVX-008	AVX-008	1	293.15	20.0	Y
1009	2011-07-27	Cal	AVX-009	Initial calibration	AVX-009	AVX-009	AVX-009	1	293.15	20.0	Y
1010	2011-07-27	Cal	AVX-010	Initial calibration	AVX-010	AVX-010	AVX-010	1	293.15	20.0	Y
1011	2011-07-27	Cal	AVX-011	Initial calibration	AVX-011	AVX-011	AVX-011	1	293.15	20.0	Y
1012	2011-07-27	Cal	AVX-012	Initial calibration	AVX-012	AVX-012	AVX-012	1	293.15	20.0	Y
1013	2011-07-27	Cal	AVX-013	Initial calibration	AVX-013	AVX-013	AVX-013	1	293.15	20.0	Y
1014	2011-07-27	Cal	AVX-014	Initial calibration	AVX-014	AVX-014	AVX-014	1	293.15	20.0	Y
1015	2011-07-27	Cal	AVX-015	Initial calibration	AVX-015	AVX-015	AVX-015	1	293.15	20.0	Y
1016	2011-07-27	Cal	AVX-016	Initial calibration	AVX-016	AVX-016	AVX-016	1	293.15	20.0	Y
1017	2011-07-27	Cal	AVX-017	Initial calibration	AVX-017	AVX-017	AVX-017	1	293.15	20.0	Y
1018	2011-07-27	Cal	AVX-018	Initial calibration	AVX-018	AVX-018	AVX-018	1	293.15	20.0	Y
1019	2011-07-27	Cal	AVX-019	Initial calibration	AVX-019	AVX-019	AVX-019	1	293.15	20.0	Y
1020	2011-07-27	Cal	AVX-020	Initial calibration	AVX-020	AVX-020	AVX-020	1	293.15	20.0	Y

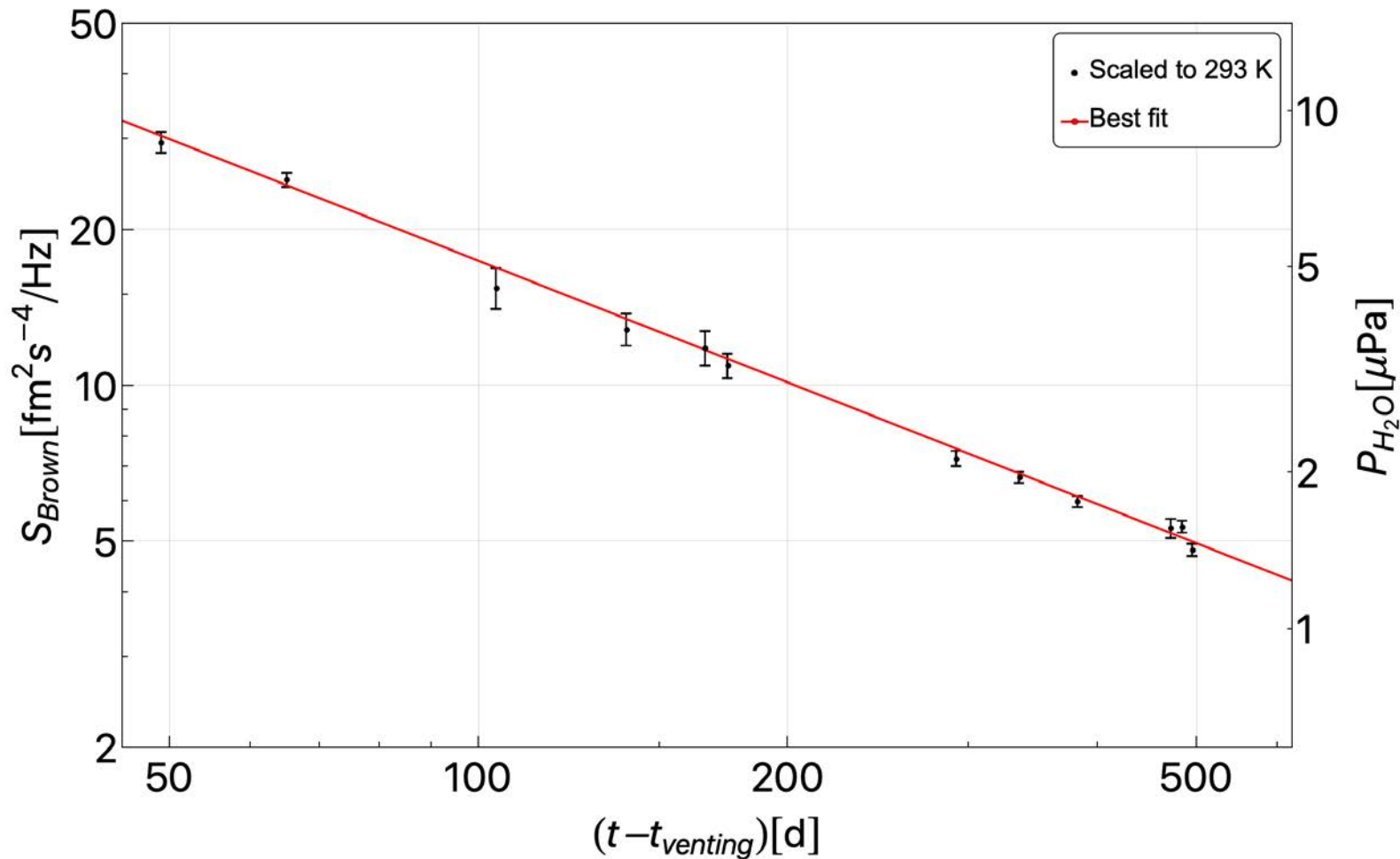
LEVEL	NAME	REMARKS	Min X [m]	Max X [m]	Min Y [m]	Max Y [m]	Min Z [m]	Max Z [m]	Min m [kg]	Max m [kg]	X cog [mm]	Y cog [mm]	Z [mm]
	New Electrode Housing										0.054419202	-6E-05	0.
	M3 HEXALOBULAR SOCKET SCREW M3x6.4 (D)	Guard ring z- screws (all)	-0.026201	0.026185	-0.026197	0.026182	-0.037475	-0.029135	1.22E-10	2.42E-08	-0.000151604	-0.0003	3
	M3 HEXALOBULAR SOCKET SCREW M3x6.4 (D)	Guard ring z- screws (all)	-0.026201	0.026185	-0.026182	0.026197	-0.029135	0.037475	1.22E-10	2.42E-08	-0.000151604	0.00033	3
	M3 HEXALOBULAR SOCKET SCREW M3x6.4 (D)	Z- cover screws (all)	-0.022529	0.022523	-0.020769	0.020756	-0.043075	-0.034735	1.23E-10	2.35E-08	-7.04325E-05	-0.0003	3
	M3 HEXALOBULAR SOCKET SCREW M3x6.4 (D)	Z+ cover screws (all)	-0.022529	0.022523	-0.020756	0.020769	0.034735	0.043075	1.23E-10	2.35E-08	-7.04325E-05	0.00027	3
	M3 HEXALOBULAR SOCKET SCREW 3X6.4 (A)	X- face screws	0.029662	0.037972	-0.030199	0.030198	-0.029194	0.029191	9.41E-11	3.64E-08	34.36440315	-0.0001	6
	M3 HEXALOBULAR SOCKET SCREW 3X6.4 (A)	X+ face screws	-0.037972	-0.029662	0.030198	0.030199	-0.029194	0.029191	9.41E-11	3.64E-08	-34.36440315	0.0001	6
	M3 HEXALOBULAR SOCKET SCREW 3X6.4 (A)	Y- face screws	-0.032203	0.032203	0.028562	0.036872	-0.030198	0.030197	9.41E-11	3.64E-08	-9.38224E-05	33.2644	0
	M3 HEXALOBULAR SOCKET SCREW 3X6.4 (A)	Y+ face screws	-0.032203	0.032203	-0.036872	-0.028562	-0.030198	0.030197	9.41E-11	3.64E-08	9.38224E-05	-33.264	0
	M3 HEXALOBULAR SOCKET SCREW 3X6.4 (A)	Z- face screws	-0.032993	0.032993	-0.032991	0.032991	-0.037472	-0.029162	9.41E-11	3.64E-08	-0.000201659	-1E-05	3
	M3 HEXALOBULAR SOCKET SCREW 3X6.4 (A)	Z+ face screws	-0.032993	0.032993	-0.032991	0.032991	0.029162	0.037472	9.41E-11	3.64E-08	-0.000201659	1.1E-05	3
	M3 HEXALOBULAR SOCKET SCREW 3X6.9 (B)	y+ dir	0.034734	0.043568	-0.019636	-0.015239	-0.006856	-0.002459	1.18E-10	2.39E-08	39.75527429	-17.436	4
	M3 HEXALOBULAR SOCKET SCREW 3X6.9 (B)		0.034734	0.043568	0.015239	0.019636	-0.006856	-0.002459	1.18E-10	2.39E-08	39.75527429	17.4358	4
	M3 HEXALOBULAR SOCKET SCREW 3X6.9 (B)		-0.043568	-0.034734	0.015239	0.019636	-0.006856	-0.002459	1.18E-10	2.39E-08	-39.75527429	17.4358	4
	M3 HEXALOBULAR SOCKET SCREW 3X6.9 (B)		-0.043568	-0.034734	-0.019636	-0.015239	-0.006856	-0.002459	1.18E-10	2.39E-08	-39.75527429	-17.436	4
	M3 HEXALOBULAR SOCKET SCREW 3X6.9 (B)	all y- cover screws	-0.011346	0.001784	0.033634	0.042468	-0.010393	0.010171	1.18E-10	2.45E-08	-3.854340843	38.6552	-
	M3 HEXALOBULAR SOCKET SCREW 3X6.9 (B)	all y+ cover screws	-0.001784	0.011346	-0.042468	-0.033634	-0.010393	0.010171	1.18E-10	2.45E-08	3.854340843	-38.655	-
	EH Frame		-0.035911	0.03592	-0.035923	0.03592	-0.034455	0.034464	1.58E-10	5.32E-07	0.168660707	-0.0001	0.
	Z+ Face Assy												

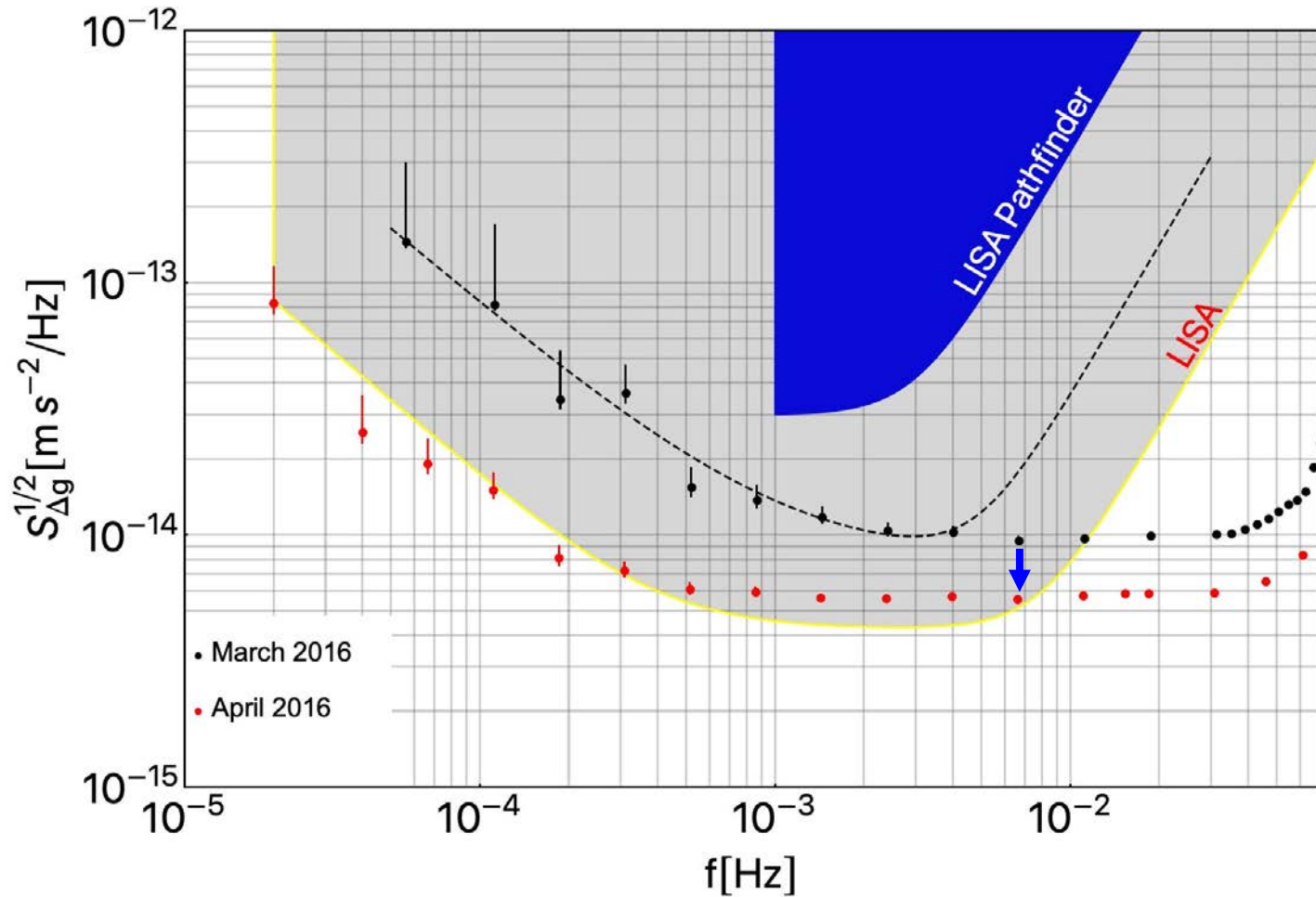




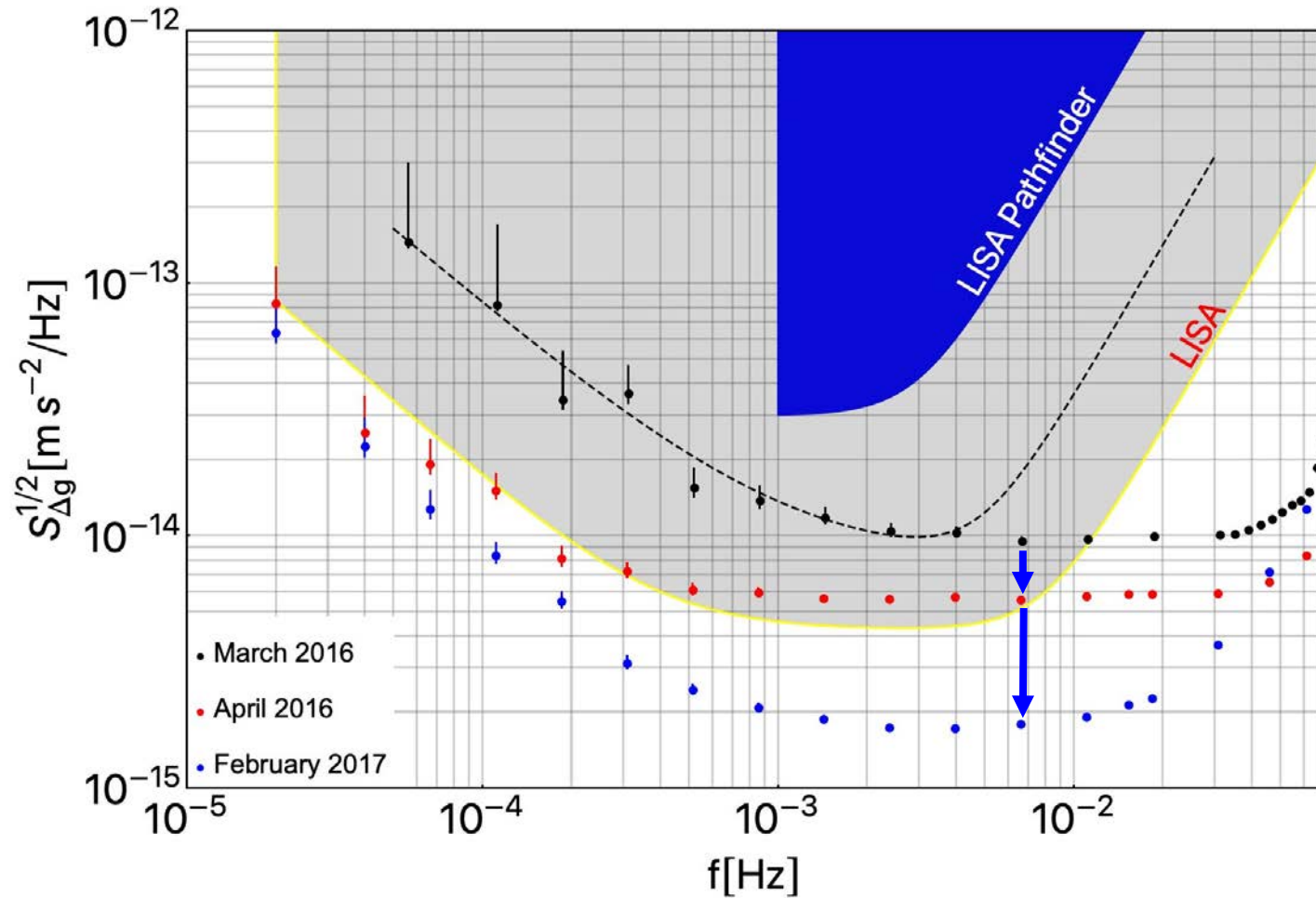


Pressure and Brownian decay





The ultimate performance



Consolidating the noise model for LISA Pathfinder full mission of experiments

In depth analysis of LISA Pathfinder performance results: time evolution, noise projection, physical models and implications for LISA

Transient acceleration events in LISA Pathfinder: properties and possible physical origin

Sensor Noise in LISA Pathfinder: An Extensive In-Flight Review of the Angular and Longitudinal Interferometric Measurement System

[1] M. Armano, et al. Sub-femto- g free fall for space-based gravitational wave observatories: Lisa pathfinder results. *Phys. Rev. D*, 93:031101, Jun 2016.

[2] D. Vetrugno et al. Lisa pathfinder first results. *International Journal of Modern Physics D*, 26(05):1741023, 2017.

[3] M. Armano, et al. Charge-induced free-falling test mass results from lisa pathfinder. *Phys. Rev. D*, 95:171101, Apr 2017.

[4] M. Armano, et al. Capacitive precision over millimeter-wide sensors. *Phys. Rev. D*, 95:031101, 2017.

[5] M. Armano, et al. Cosmic-ray flux and energy dependence of galactic cosmic-ray flux and of a forburst. *The Astrophysical Journal*, 854(2):113, Feb 2018.

[6] M. Armano, et al. Performance: New lisa pathfinder noise floor down to 20 μHz . *Phys. Rev. D*, 120:061101, Feb 2019.

[7] M. Armano, et al. Calibrating the dynamics of lisa pathfinder. *Phys. Rev. D*, 98:062001, Jun 2018.

[8] M. Armano, et al. Precision charge control for isolated free-fall. Lisa pathfinder results. *Phys. Rev. D*, 98:062001, Sep 2018.

[9] G. Anderson, et al. Experimental results from the mission on lisa pathfinder. *Phys. Rev. D*, 98:102005, Nov 2018.

[10] M. Armano, et al. Forbush decreases and <2 day GCR non-recurrent variations studied with LISA pathfinder. *The Astrophysical Journal*, 874(2):167, Apr 2019.

[11] M. Armano, et al. Lisa pathfinder platform drag-free performance. *Phys. Rev. D*, 99:082001, Apr 2019.

[12] M. Armano, et al. Temperature control in the sub-milliHertz band with LISA pathfinder. *Monthly Notices of the Royal Astronomical Society*, 486(3):3368–3379, 04 2019.

[13] M. Armano, et al. Characterization of microneutron cold gas thrusters: In-flight characterization. *Phys. Rev. D*, 99:122003, Jun 2019.

[14] M. Armano, et al. Lisa pathfinder performance confirmed in an open-loop configuration. Results from the free-fall actuation mode. *Phys. Rev. Lett.*, 123:061101, 2019.

[15] M. Armano, et al. Micrometeoroid events in LISA pathfinder. *The Astrophysical Journal*, 883(1):53, Sep 2019.

[16] M. Armano, et al. Novel methods to measure the gravitational constant in space. *Phys. Rev. D*, 100:062003, Sep 2019.

[17] M. Armano, et al. Analysis of the accuracy of actuation electronics in the laser interferometer space antenna pathfinder. *Review of Scientific Instruments*, 91(4):045003, 2020.

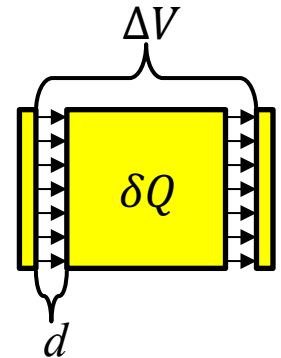
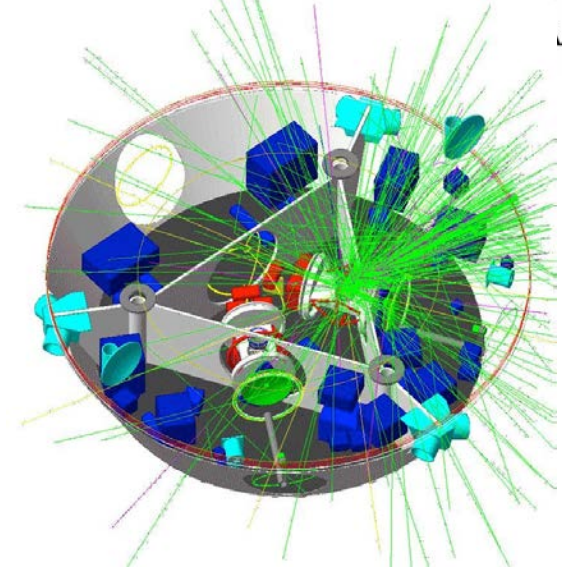
[18] M. Armano, et al. Spacecraft and interplanetary contributions to the magnetic environment on-board LISA Pathfinder. *Monthly Notices of the Royal Astronomical Society*, 494(2):3014–3027, 04 2020.

[19] M. Armano, et al. Sensor noise in lisa pathfinder: In-flight performance of the optical test mass readout. *Phys. Rev. Lett.*, 126:131103, Apr 2021.

Test mass charging

[3] M. Armano, et al. Charge-induced force noise on free-falling test masses: Results from lisa pathfinder. *Phys. Rev. Lett.*, 118:171101, Apr 2017.

- Cosmic rays keep charging up the test-mass
 - Random charge δQ interact with parasitic potentials ΔV and produces force noise
- $$\delta F_Q = \frac{\delta Q \Delta V}{d}$$
- Charging events random and uncorrelated: Poisson statistics expected.
 - Force noise with $1/f$ spectrum

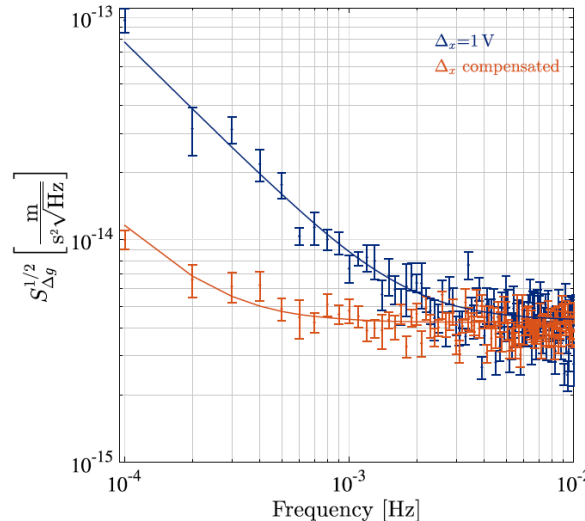
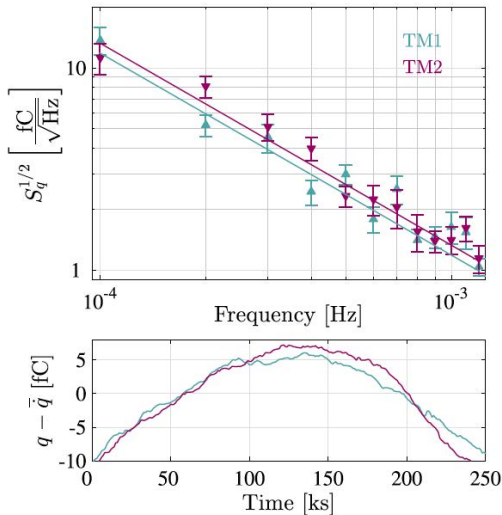
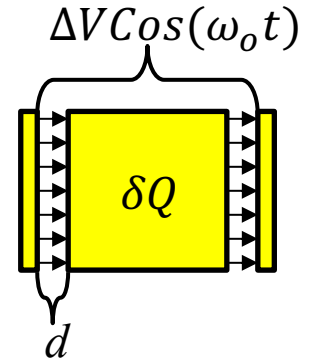


Test mass charging

- We were able to measure charge by using an oscillating potential
- Oscillating force produced

$$\delta F_Q = \frac{\delta Q}{d} \Delta V \cos(\omega_0 t)$$

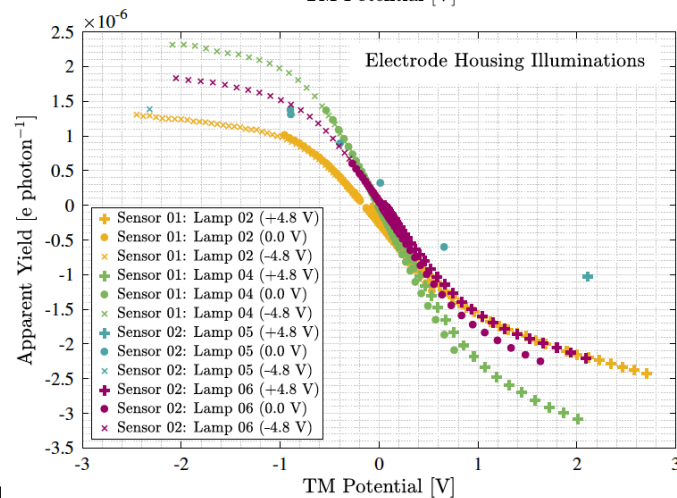
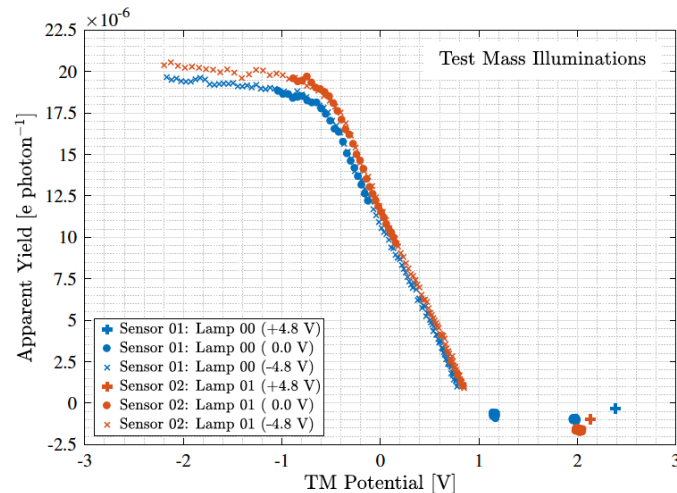
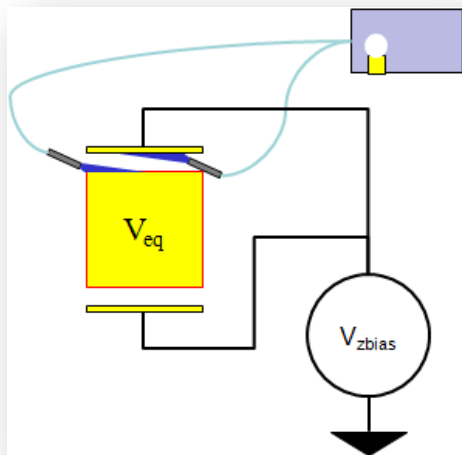
- $\delta Q(t)$, at frequencies $\ll \omega_0/2\pi$, from induced test-mass motion



Suppressing force noise due to charge by balancing the parasitic potential

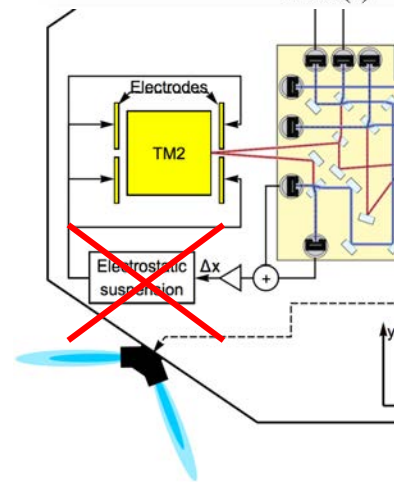
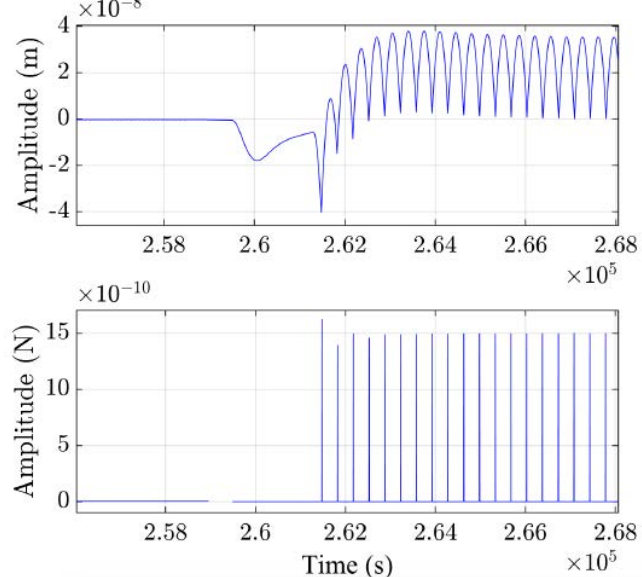
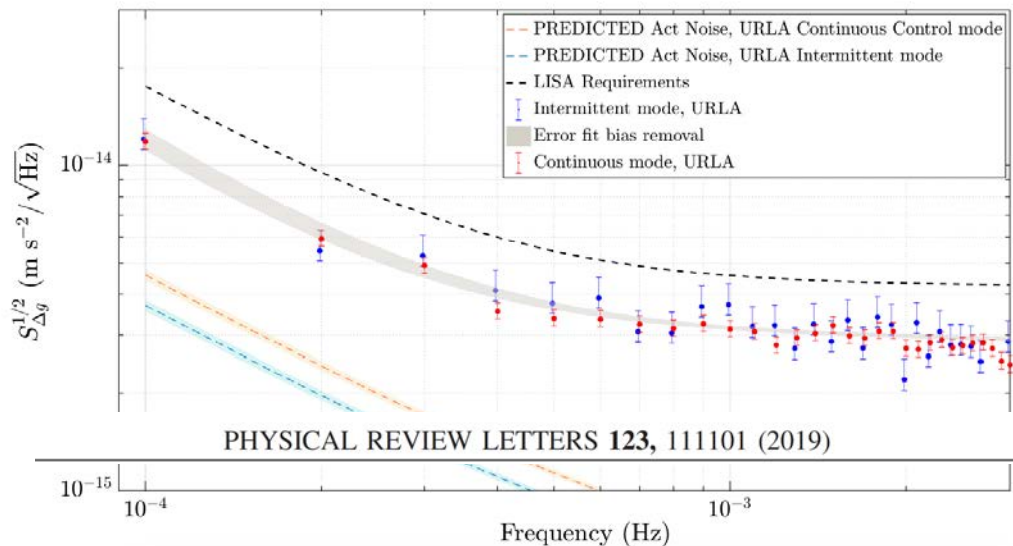
Test mass discharging

- Charge biases TM and needs to be removed
- Discharging performed with UV light (non contacting)
- Electron can both be extracted from TM or deposited onto it
- Full bipolar discharging achieved

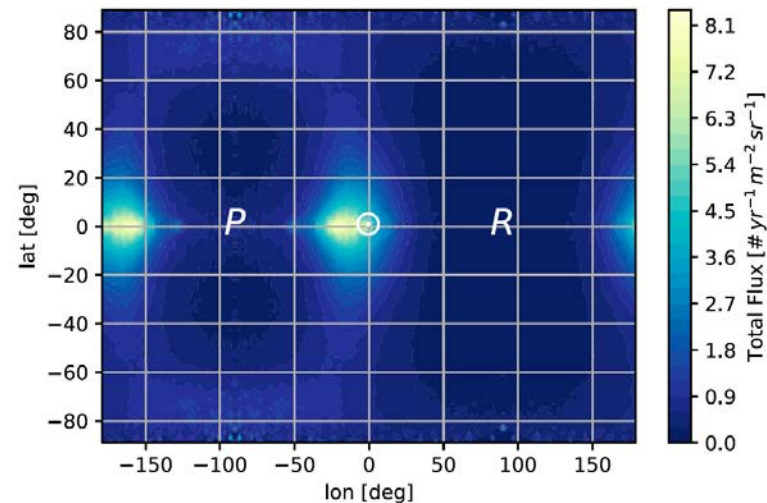
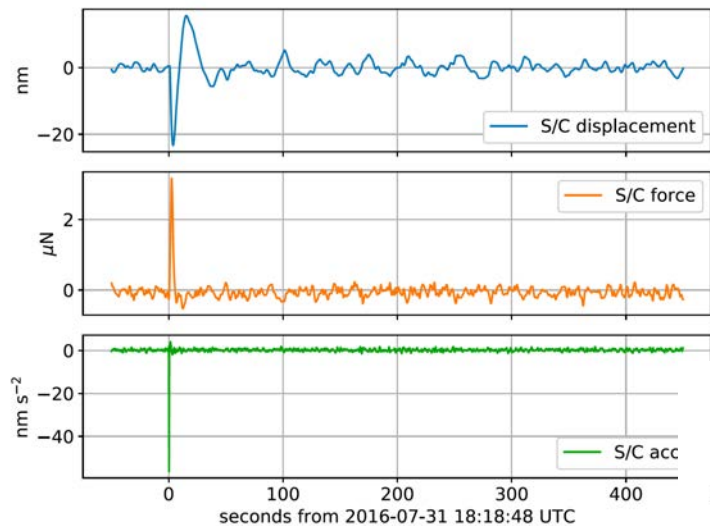


An independent check of performance: gravimeter vs accelerometer

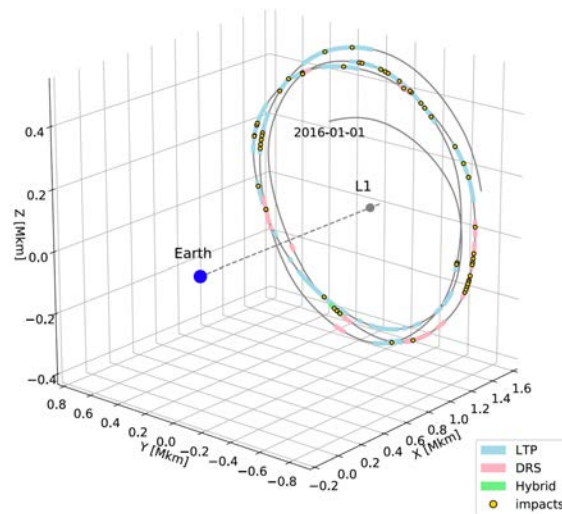
- Control with intermittent force pulses and unperturbed 300 s flights in between
- Noise on time scale > 300 s accurately interpolated



Micrometeroid impacts on LPF

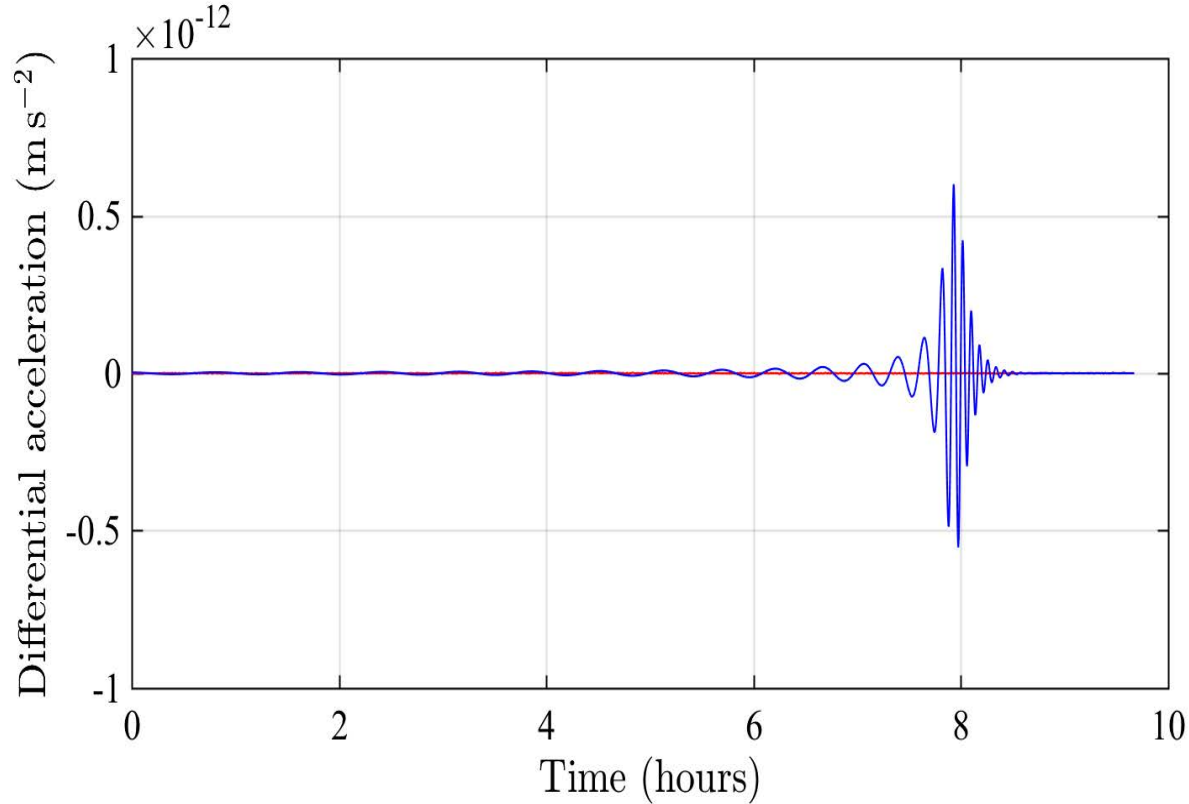


(a) Jupiter-Family Comets (JFC)



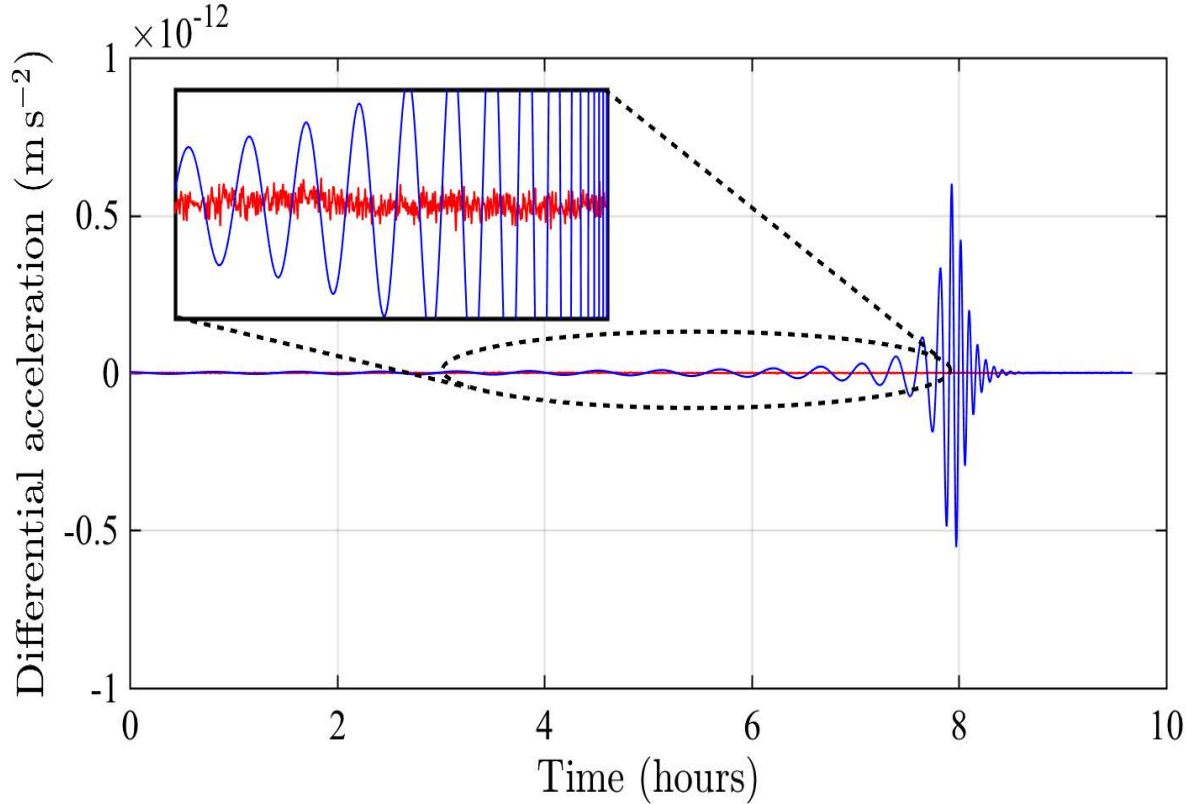


LISA Pathfinder acceleration data





LISA Pathfinder acceleration data





NEWS

Home Video World UK Business Tech Science Stories Entertainment & Arts



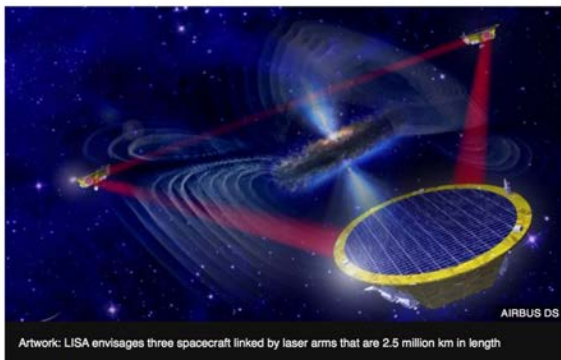
Science & Environment

Europe selects grand gravity mission

By Jonathan Amos
BBC Science Correspondent, Paris

© 20 June 2017

f t b e Share



Artwork: LISA envisages three spacecraft linked by laser arms that are 2.5 million km in length

Green Light for LISA

ESA Unclassified – For official use

ESA/SPC/MIN/154, rev.1 (Final)
Att.: Annex
ESA/SPC/OJ/154, rev.1 (Final)
Paris, 29 March 2018
(Original: English)

EUROPEAN SPACE AGENCY

SCIENCE PROGRAMME COMMITTEE

One hundred and fifty-fourth meeting,
held at ESAC, in Villanueva de la Cañada on 20 and 21 June 2017

Minutes, as approved during the 155th meeting held on 21 and 22 November 2017

Chair: Mr J. Christensen-Dalsgaard (Denmark)
(Participants: see Annex)

The Committee unanimously selected (with Greece in writing) the LISA mission for the L3 flight opportunity, with a planned launch date in 2034, and with an estimated CaC of €1.05b (at 2017 e.c.).

Phase A Conclusions – MFR outcome

Timeline



October 2013:
 October 2016:
 June 2017:
 May 2018:
2018-2021:
Oct '20-Oct '21:

April 2022 Phase B1 Kick-Off (New Requirements Architecture ready)

6. C Q4 / 2022 Intermediate Review (Consolidation of requirements to CFIs)

The bridg the b **Q2 / 2023** Instrument SRR (“Adoption review for CFIs”) d of the e end of

~~Q4 / 2023~~ Mission Adoption Review **Q3 2023**

The the p ~~Q1 / 2024~~ Mission **Adoption (TBC)** **Q4 2023** well as sortium.

The The ... participants for their valuable contributions to the Review.

<end 2021: Formulation Review (end Phase A)

>2021: Mission Phase B1

<2024: Mission Adoption

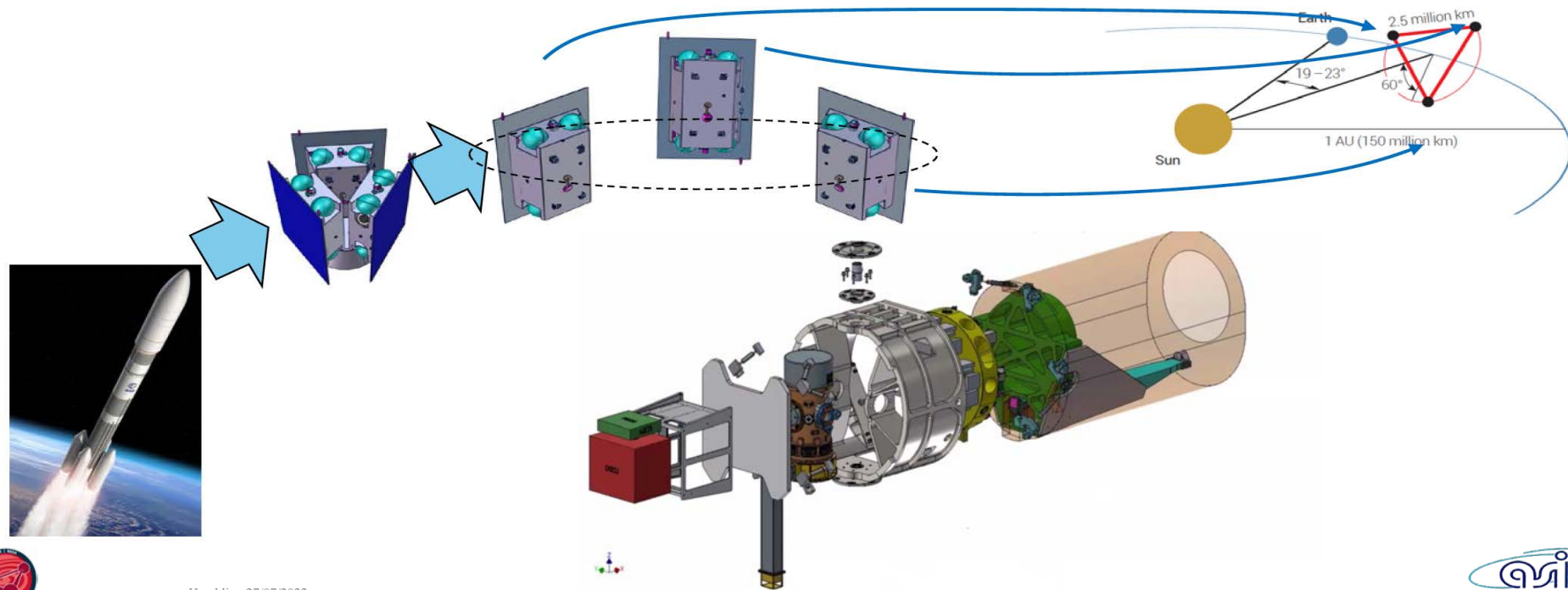
>Adoption: Mission Implementation (Phase B2/C/D)

<2034: Launch

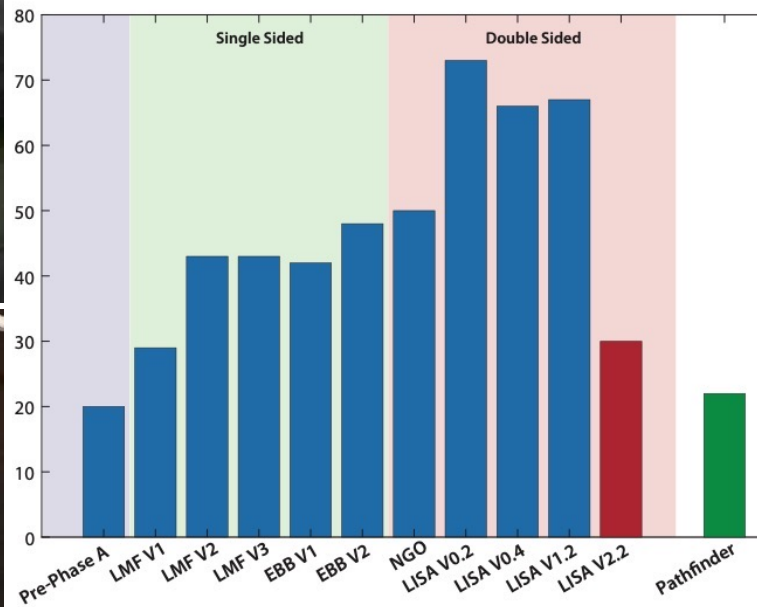
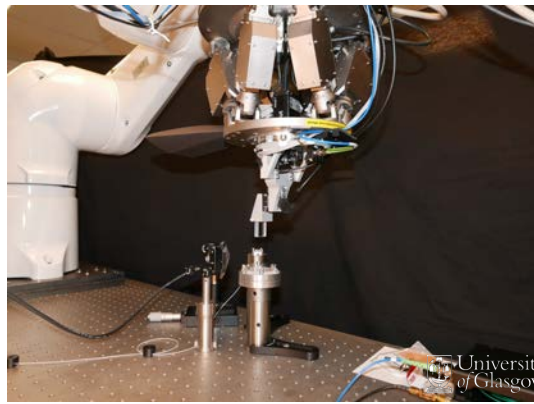
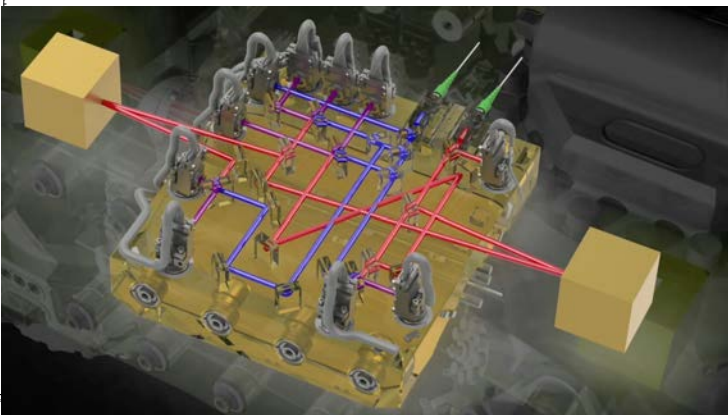
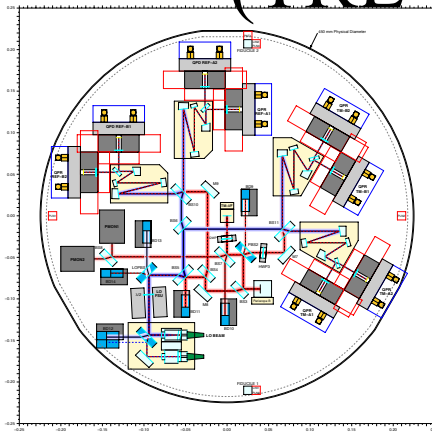
>Launch: 6.5 years operations (+6 years potential extension)

LISA currently in phase B1

- Phase-A study competitive: cannot show much!
- A rather stable concept, working out the details



Technology developments (TRL 6 by adoption)



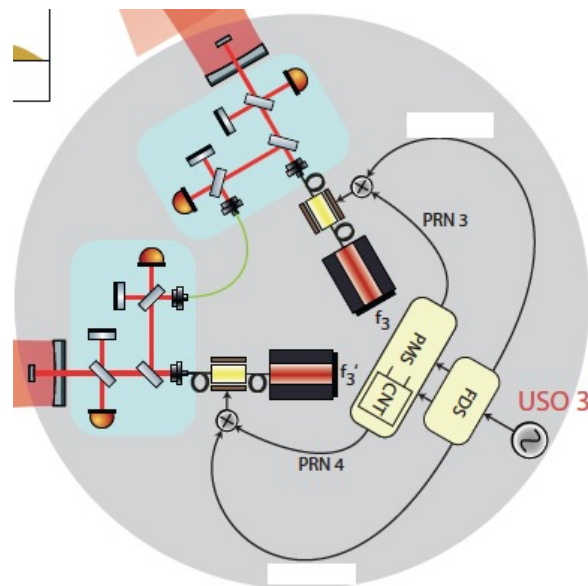
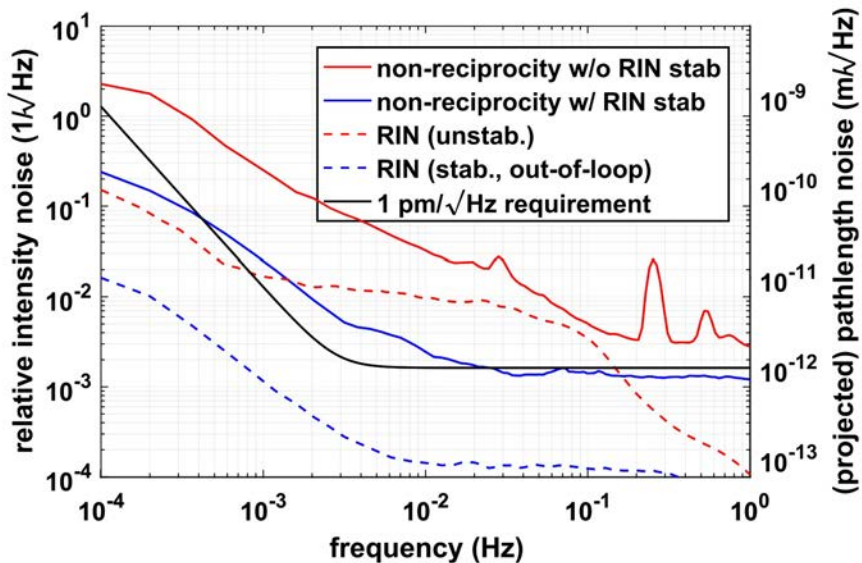
Technology developments (TRL 6 by adoption)



- The back link systems

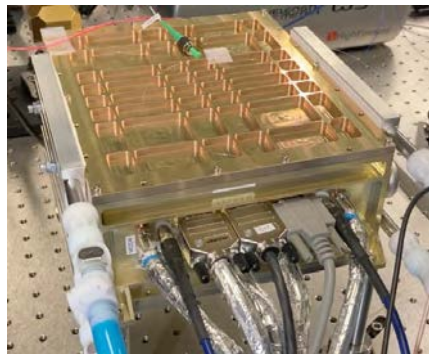
Class. Quantum Grav. 35 (2018) 075007

R Fleddermann *et al*



rsity
gow

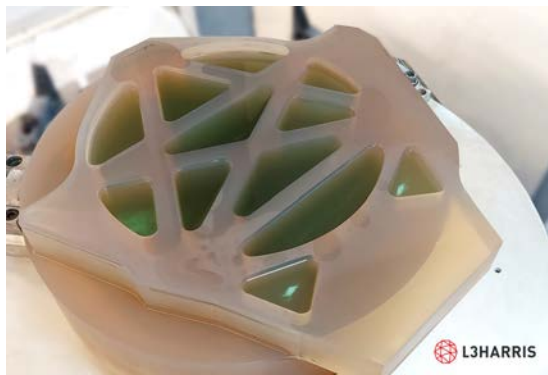
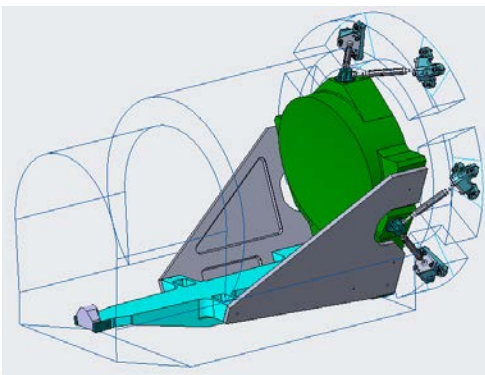
Technology developments (TRL6 by adoption)



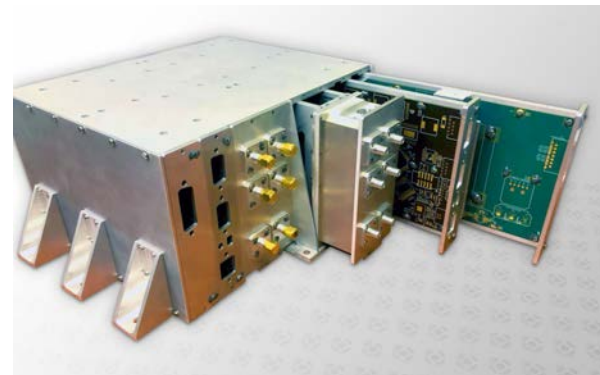
Laser



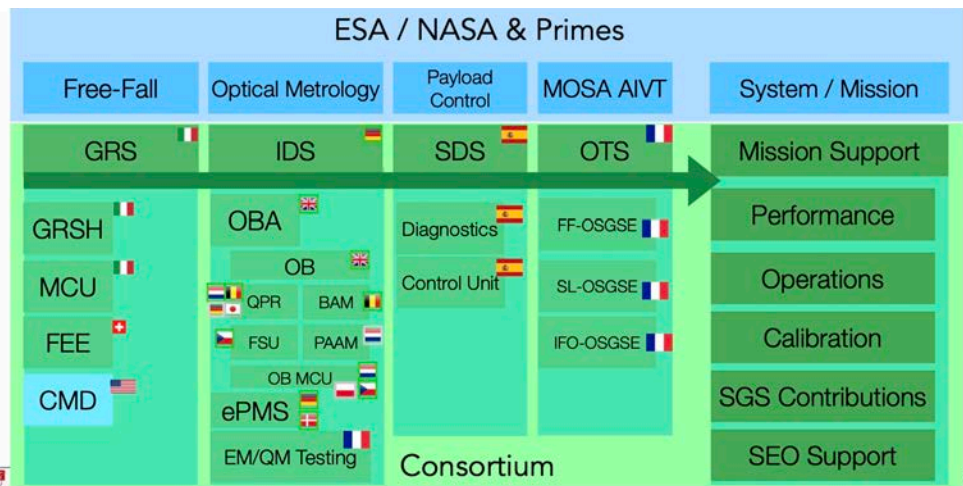
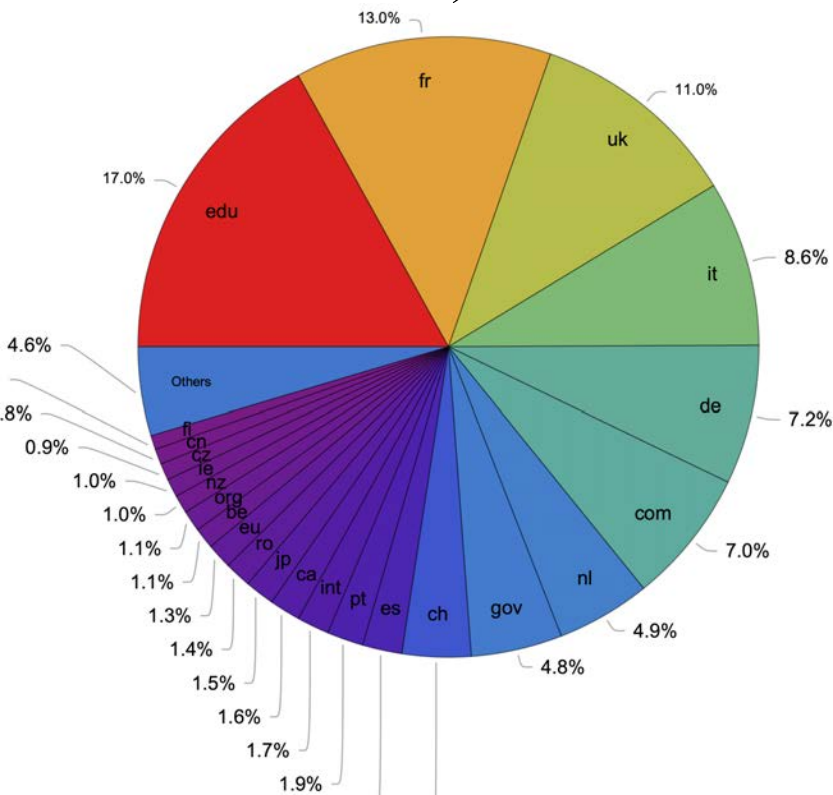
Telescope



Charge management



- The LISA Consortium (1437
1612 members)



University of Glasgow
UK Astronomy Technology Centre

LISA SYMPOSIUM XIV

25th - 29th July 2022

Virtual Conference

LISA Symposium 2022

The main LISA Symposium website is hosted by OxfordAbstracts.com.

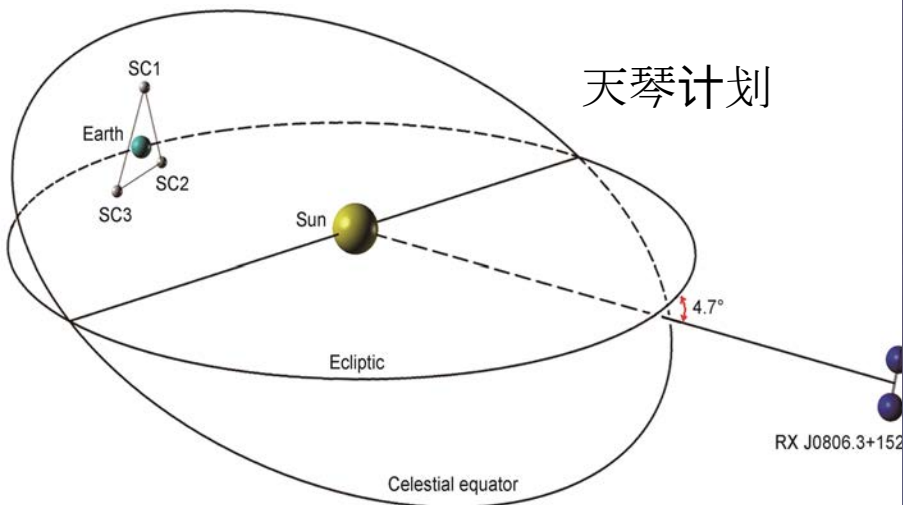
[Click here to register](#)

You will need to create an Oxford Abstracts account to register for the Symposium.

[Link to main event website](#)

Beyond and besides LISA

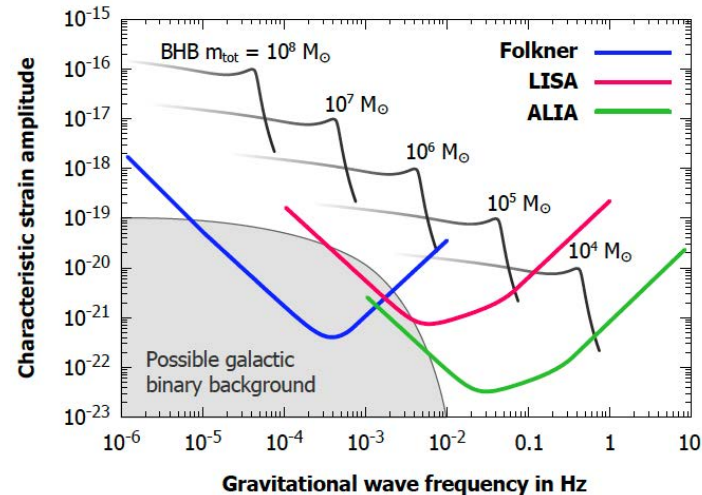
- Efforts in China



Beyond and besides LISA

- Planning for the future

- **New Physical Probes of the Early Universe.** How did the Universe begin? How did the first cosmic structures and black holes form and evolve? These are outstanding questions in fundamental physics and astrophysics, and we now have new astronomical messengers that can address them. Our recommendation is for a Large mission deploying gravitational wave detectors or precision microwave spectrometers to explore the early Universe at large redshifts. This theme follows the breakthrough science from *Planck* and the expected scientific return from *LISA*.





Thank you!

MUSE

MUSE

MUSE